THE PRINCIPLES AND ANALOG STUDIES OF AN IDEAL VIBRATION DAMPER

C. G. ERB

S. S. COX

THE PRINCIPLES AND ANALOG STUDIES OF AN IDEAL VIBRATION DAMPER

by

Charles G. Erb, Lieutenant, U.S. Navy
B.S., U.S. Naval Postgraduate School, 1956

Sidney S. Cox, Lieutenant, U.S. Navy
B.S., U.S. Naval Academy, 1949
B.S., U.S. Naval Postgraduate School, 1956

SUBMITTED IN PARTIAL FULFILLMENT OF THE

REQUIREMENTS FOR THE DEGREE OF

MASTER OF SCIENCE

at the

MASSACHUSETTS INSTITUTE OF TECHNOLOGY

1957

This thesis, written by the authors while affiliated with the Instrumentation Laboratory, M.I.T., has been reproduced by the offset process using printer's ink in accordance with the following basic authorization received by Dr. C. S. Draper, Head of Department of Aeronautical Engineering and Director of the Instrumentation Laboratory.

COPY

March 1, 1956

Dr. C. S. Draper
Head of the Department of Aeronautical Engineering
and Director of the Instrumentation Laboratory

Dear Dr. Draper:

This is to authorize the deposit in the Library of permanent, offset-printed copies of theses published by the Instrumentation Laboratory in lieu of the ribbon copies normally required.

THE PRINCIPLES AND ANALOG STUDIES OF AN IDEAL VIBRATION DAMPER

by

Charles G. Erb
Sidney S. Cox

Submitted to the Department of Aeronautical Engineering on May 20, 1957, in partial fulfillment of the requirements for the degree of Master of Science.

ABSTRACT

The perfect damper for vibration isolation produces damping force proportional to and always opposing the "absolute" velocity of the body to be isolated with respect to an established inertial reference. The established inertial reference is defined by the average velocity of the support over a specified period of time preceding a disturbance. When the damper is attached to this inertial reference, it will always remove energy of the "absolute" motion from the body.

In an actual case, however, one end of the damper is usually attached to the support and the damping force is proportional to the instantaneous relative velocity of the support with respect to the body. This force is not always opposing the "absolute" motion of the body. Consequently, energy is alternately being added and subtracted from the body.

Professor Y. T. Li has devised a nonlinear system for ideal damping such that when energy is being added to the body, the coefficient of damping is small, resulting in a minimum of energy transfer. When energy is being subtracted from the body, the damping coefficient is large, resulting in maximum energy

transfer. By employing this idea, the performance of a perfect damper can be approached.

Control of the damping coefficient with respect to energy transfer is based on a comparison of the "absolute" and relative velocities. When the velocities, as defined, are of the same algebraic sign, energy is being added to the body, hence the lower damping coefficient is selected. When the velocities are of opposite signs, the higher damping coefficient is utilized since energy is now being removed. This establishes a criterion for the control of the damping force.

To verify the theory, a nonlinear electronic analog was devised and tested and a mechanical analog was designed. The results were consistent with the theory.

Thesis Supervisor: Y. T. Li

Title: Associate Professor of Aeronautical Engineering

ACKNOWLEDGMENTS

Grateful acknowledgment is made to Professor Y. T. Li for his invaluable advice in all aspects of this thesis; to Mr. Richard P. Lucius, Jr., for his technical assistance in electronics; to Mr. Sidney A. Wingate for his assistance in the design of the electronic switch; and to Mr. John Barley for his technical assistance in the construction of the mechanical model.

The graduate work for which this thesis is a partial requirement was performed while the authors were assigned to the U. S. Naval Administrative Unit, Massachusetts Institute of Technology, Cambridge 39, Massachusetts.

TABLE OF CONTENTS

LIST OF ILLUSTRATIONS

CHAPTER 1

INTRODUCTION

Consider the vibration of a body as being induced by motions of its support. For a linear coupling system in which only a spring couples the body and support, the dynamic performance under certain operating conditions results in large amplitude ratios. These conditions exist after the occurance of a step displacement of the support and result in transient oscillations, or when the support displacement oscillates with a frequency in the region of the system natural frequency The primary purpose of a damper is to reduce these large amplitude ratios, thus tending to effect vibration isolation.

Perfect damping is attained only when the damper is connected between the body and an inertial reference In conjunction with the spring between body and support, this coupling system provides a damping force on the body always generated in opposition to the "absolute" motion of the body. In the practical coupling system, however, the damper is connected in parallel with the spring between the body and support, and the damping force is generated by the relative velocity. Since this force is not always opposite to the absolute motion, the damping is inferior to that of a perfect damper. Perfect damper performance is presented in Fig. 1.1.

In general, the design of a vibration isolation system involves many complex problems (1)*, (2), (3), consequently "The

* Underlined numbers in parenthesis refer to Bibliography.

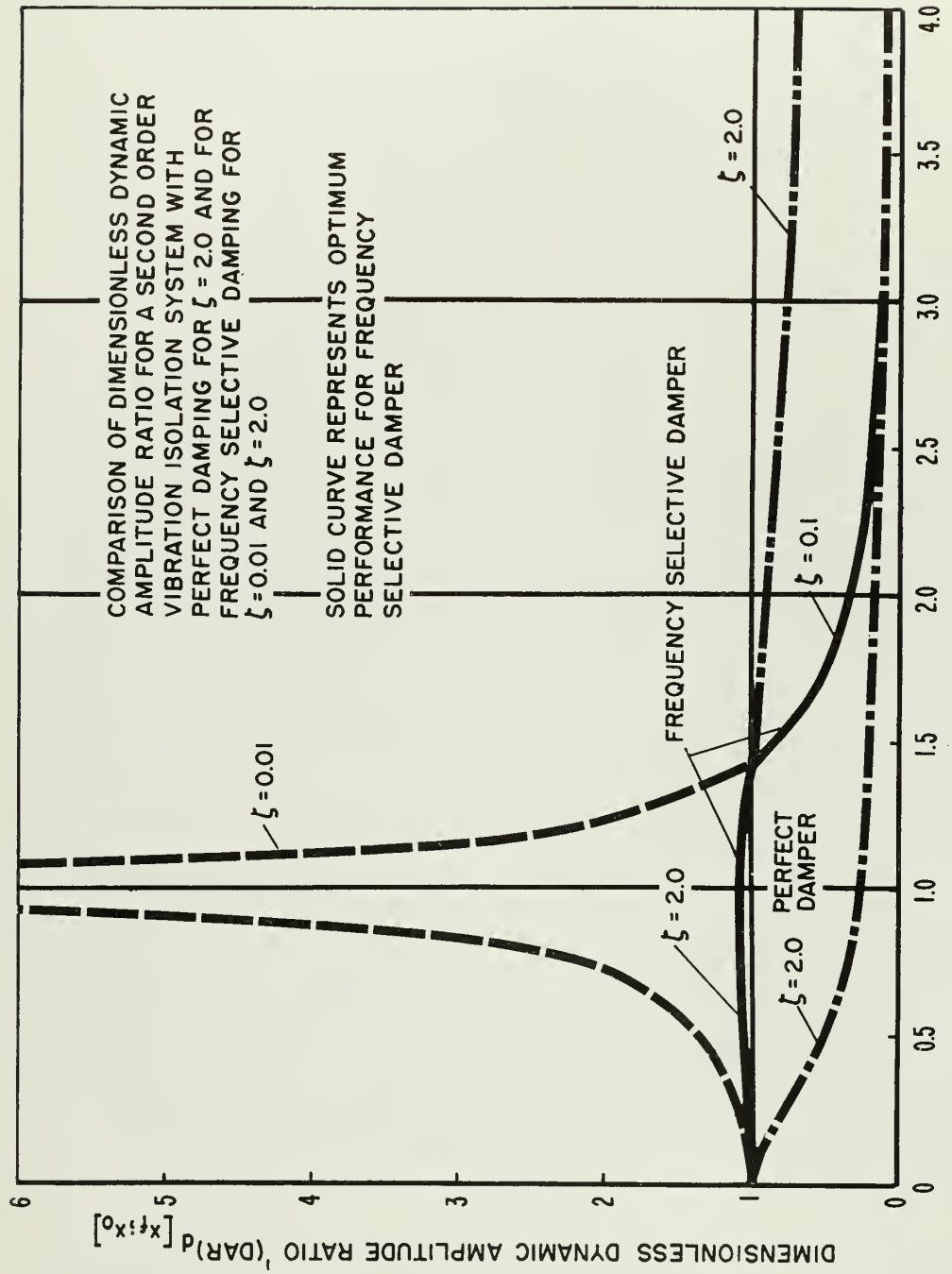

Fig. 1-1 Typical System Frequency Response Amplitude Ratios; Frequency-Selective Damper, and Perfect Damper

approach to the damping problem has been more experimental than theoretical in the past." (4). Recently there has been an endeavor to reduce these problems to understandable parameters and design criteria (5).

Most of the improvements in dampers have been compromises between optimum performance in a normal operating range and the adverse performance outside this range. Two exceptions are notable. A recent proposal (6) incorporates a frequency-sensitive control of the damping action so as to take advantage of the best performance of either a high or a low coefficient of damping as determined by the frequency of the support motion relative to the natural frequency. A typical optimum frequency-response performance by this method is presented in Fig. 1.1, which is shown as compared to a system with perfect damping. The other exception is an early design (7) of an automobile damper which used the inertia of a mass to provide limited control of the damping force. Transient response data is reproduced in Fig. 1.2. No frequency response data was available in the literature. The nonlinearity of this damper operation was such that the magnitude of the damping force, while necessarily proportional to the relative velocity, was large when it opposed the absolute motion of the body and small when it did not oppose. However, the damping force in this particular design was controlled only during the time when the relative support motion was downward. This design clearly illustrated that engineers were familiar with the problem, but apparently the concept of using an inertial mass to control the damping was not fully understood.

In an inertial mass controlled damper, the control element can be designed to be either acceleration or velocity dependent. The design in (7) appears to be based on the assumption that the undesired acceleration of the body was due solely to forces applied through the damper and that if the magnitude of this force

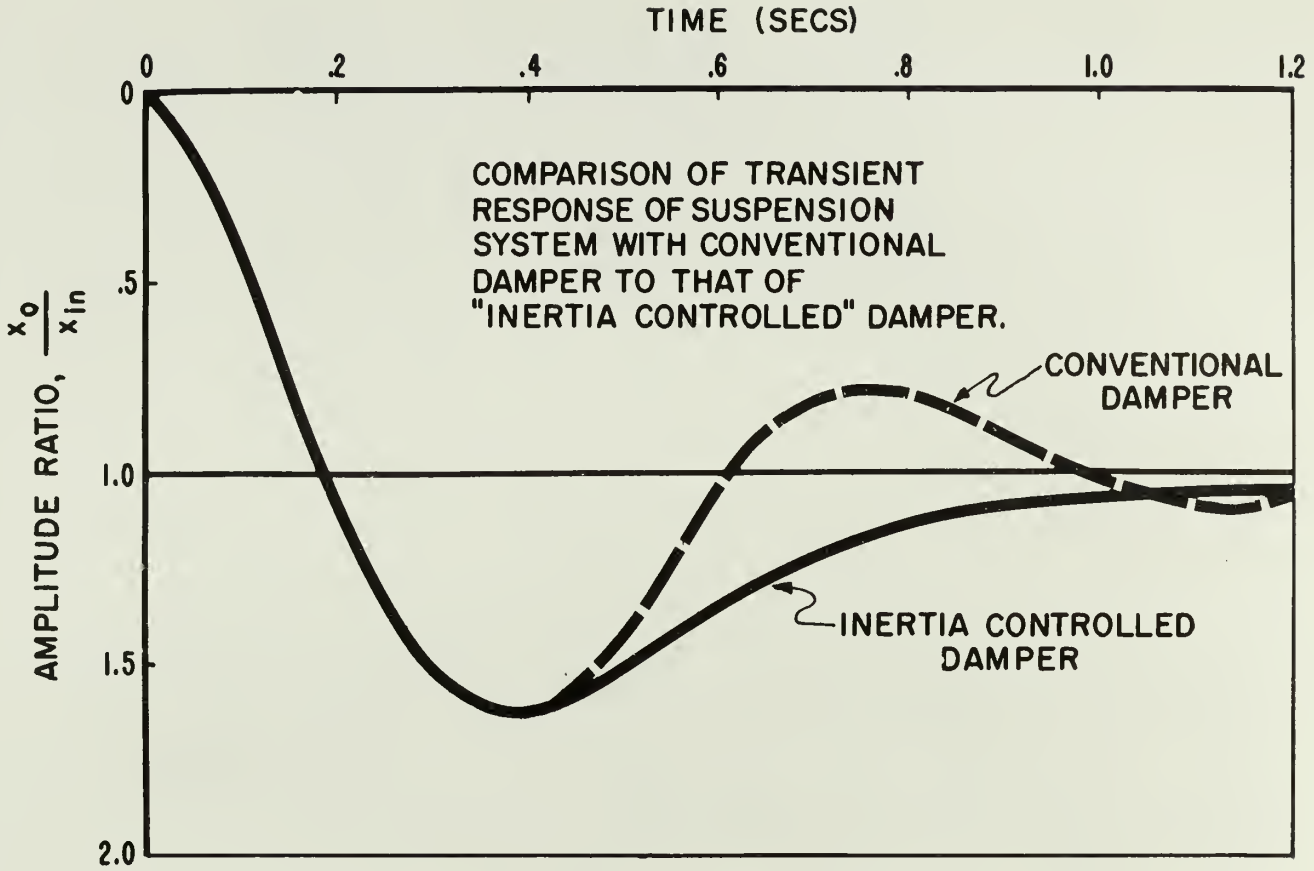

Fig. 1-2 Transient Response Amplitude Ratios of Automobile Suspension System with Conventional Damper, and with Early "Inertia Controlled" Damper

could be judiciously controlled, the adverse accelerations could be reduced. This was a correct approach if the only force applied to the body was the damping force. This was not the case, however, in that an automobile suspension system includes a spring which applies a force to the body not necessarily in phase with the damping force. Therefore, the force applied by the spring must be considered when determining a criterion for the control of the damping force. This was not considered in the inertia controlled damper. Force supplied by a damper is alternately adverse and desirable, and in the control of this force, all factors must be considered.

In order to properly control damping force, Professor Li* has developed a criterion for ideal damping based on the "absolute" velocity of the body to be isolated from vibration and the relative velocity of this body with respect to its support. The damping force is necessarily proportional to the relative velocity but the magnitude of the proportionality constant can be controlled, thus controlling the force. It is desired that the damping force be small when in phase with the "absolute" velocity of the body, and large when out of phase with it.

Professor Li has proposed a single-degree-of-freedom piston-type damper in which the damping is dependent on the alignment of two concentric ported sleeves mounted on and concentric to the damper piston, and through which the damping fluid must flow when passing from one side of the piston to the other. When the ports are not aligned, a high coefficient of damping exists; when the ports are aligned, only a low residual coefficient of damping exists.

The criterion for misalignment (large coefficient of damping) is that the direction of the "absolute" velocity, obtained by a velocimeter, must be opposite to the direction of the relative

---

* Y. T. Li, Professor, Aeronautical Engineering Department, M.I.T., Cambridge, Massachusetts.

velocity. Relative velocity is herein defined as the velocity of support with respect to the body.

In discussing "absolute" velocity of a transported body, the inertial reference must be modified to allow the body to follow a desired curved path. Since an inertial reference may be defined as the average of the instantaneous inertial velocities existing within a certain time period, a modified inertial reference is so defined for a short period of time preceding the occurance of a disturbance. As an example, an automobile would use a time period of several seconds. Effectively, this modified inertial reference is a function of desired body velocity with respect to which any other velocity is considered as undesirable vibration. Thus "absolute" velocity herein denotes this vibration velocity.

This investigation was to verify the system and determine the dynamics of this damper.

To verify the system, an electronic analog was devised consisting of a second-order differential equation of the (1, 0; 0, 1, 2) type. The low coefficient of residual damping was always active in the system; a parallel high coefficient of additional damping was active only when an electronic switch, suggested by S. A. Wingate*, was "on". This occurred when the criterion was met as determined from the signs of the velocities involved.

The system was verified electronically, and an experimental model was designed. Notations used correspond to those of (9).

---

* Sidney A. Wingate, Director of Research, GPS Instrument Co., Boston, Massachusetts.

CHAPTER 2

PRINCIPLES OF AN IDEAL VIBRATION DAMPER

Consider a body attached to a vibrating support. If it is desired to minimize vibration transmission, a spring is used for the coupling. This system is only effective above the resonant frequency region. Near resonance, large amplitude ratios result. Energy dissipation in the form of damping is utilized to reduce the amplitude ratio in the resonant frequency region, but this decreases the effectiveness of the spring at high frequencies.

The conventional spring and damper configuration is shown in Fig. 2-3(a) and is represented by the following second-order differential equation obtained by equating a summation of forces on the mass to zero.

$$\begin{pmatrix}\text{inertia}\\ \text{reaction}\\ \text{force}\end{pmatrix} + \begin{pmatrix}\text{viscous}\\ \text{damping}\\ \text{force}\end{pmatrix} + \begin{pmatrix}\text{elastic}\\ \text{force}\end{pmatrix} = 0 \quad (2\text{-}1)$$

$$- m\ddot{x}_o + C_d\dot{x}_r + k x_r = 0$$

where: $x_r = (x_{in} - x_o)$

A perfect damper would not connect the body to its support but rather to a modified inertial reference. (This modified inertial reference is described later in this chapter.) The resulting damping force always opposes any velocity of the body. This configuration is shown in Fig. 2-3(b) and is represented by the following second-order differential equation:

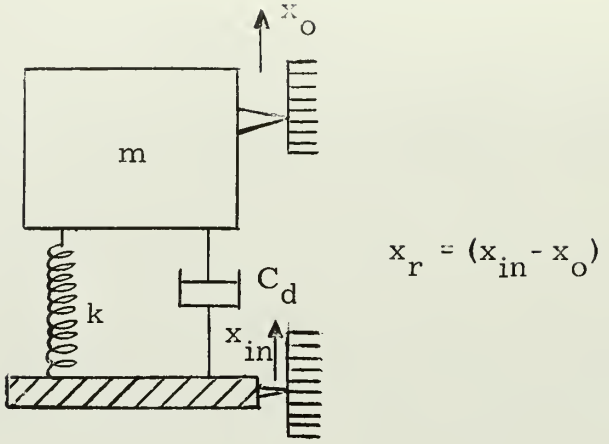

Fig. 2-3(a) Conventional Spring and Damper Configuration For Vibration Isolation

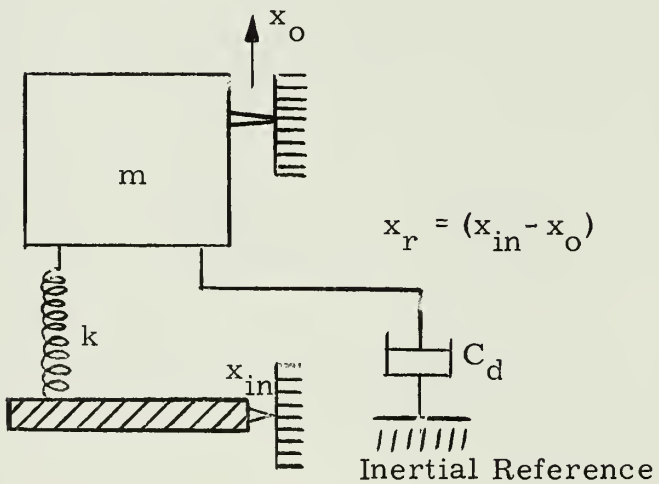

Fig. 2-3(b) Spring and Damper Configuration To Obtain Perfect Damping In Vibration Isolation System

$$- m\ddot{x}_o - C_d\dot{x}_o + kx_r = 0 \qquad (2\text{-}2)$$

The perfect damper decreases the amplitude ratio more effectively at resonant frequencies and actually improves the performance of the spring-only system at high frequencies. Typical frequency response curves for the three systems are shown in Fig. 2-4.

Perfect damping is not physically realizable since generally no inertial reference exists to which the damper may be attached. Conventionally, the damper is connected to the support and damping force must be based on the relative velocity, resulting in the performance limitations described above. These limitations result from the fact that the damping force is sometimes in phase with, and thus not opposing, the velocity of the body.

Professor Li has devised a method, based on relative velocity, for approaching perfect damping whereby the magnitude of the damping coefficient C_d is controlled, thus controlling the force. When the force from this nonlinear damper is adding energy to the body, a small value of C_d is utilized. The adverse force still exists but is minimized. When the damping force is subtracting energy, a large C_d is utilized, and a maximum desirable force is applied. A small residual damping coefficient, $C_{d(res)}$, is always present in the nonlinear damper, but an additional damping coefficient $C_{d(add)}$ is introduced when energy is being removed. The performance of this damper approaches that of the perfect damper.

In order to control the C_d, it must be established just when energy is being removed and during that time inject the $C_{d(add)}$. A criterion for introduction of $C_{d(add)}$ must be determined. When the "absolute" velocity of the body ($\dot{x}_o$) is in a direction opposite to the damping force, energy is being removed. Since the direction of the damping force on the body is in the direction of the relative velocity of the support with respect to the body

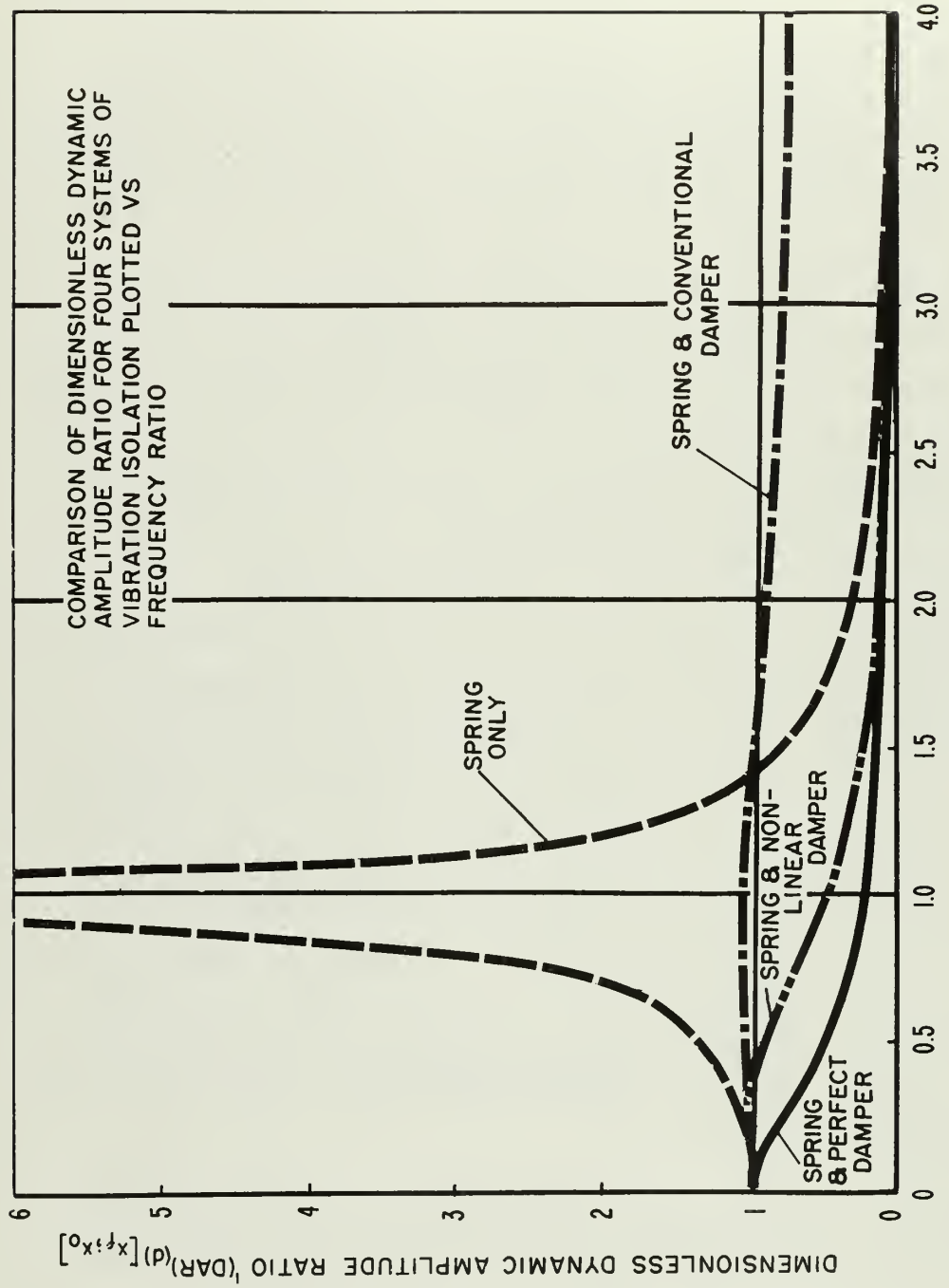

Fig. 2-4 Typical System Frequency Response Amplitude Ratios; Spring Only, Spring and Conventional Damper, Spring and Perfect Damper, and Spring and Nonlinear Ideal Damper

($\dot{x}_r = \dot{x}_{in} - \dot{x}_{out}$), the criterion is that the algebraic sign of the "absolute" velocity must be opposite to that of the relative velocity. The additional-damping-force (adf) control criterion is summarized below.

Output Velocity ($\dot{x}_o$)	Relative Velocity $\dot{x}_r = \dot{x}_{in} - \dot{x}_{out}$	Damping Force $C_d \dot{x}_r$	C_d
+	-	Desirable	$C_{d(res)} + C_{d(add)}$
+	+	Adverse	$C_{d(res)}$
-	-	Adverse	$C_{d(res)}$
-	+	Desirable	$C_{d(res)} + C_{d(add)}$

A method for the actual control of C_d is presented in Chapter 4 for both the electronic analog and the mechanical piston-type damper.

The inertial reference previously mentioned for the perfect damper must be modified for a practical damper to allow for gradual changes of the support velocity. Since these gradual changes are not undesirable, the inertial reference is defined by the average velocity of the support over a specified interval of time preceding any disturbance.

As an example, consider an automobile traveling up a corrugated ramp. Several seconds are required after engaging the ramp to establish the average velocity of the wheels corresponding to the average slope of the ramp, thus establishing a modified inertial reference. Only the motion of the body with respect to this modified inertial reference constitutes vibration. The nonlinear equation of motion for the ideal damper is:

$$- m\ddot{x}_o + \left[C_d(\dot{x}_{in} - \dot{x}_o)\right] + k(x_{in} - x_o) = 0 \qquad (2\text{-}3)$$

where: $C_d = C_{d(res)}$ when $\dot{x}_o$ and $(\dot{x}_{in} - \dot{x}_o)$ have same sign

$C_d = C_{d(res)} + C_{d(add)}$ when $\dot{x}_o$ and $(\dot{x}_{in} - \dot{x}_o)$ have opposite signs

A graphical solution to this equation is discussed in Appendix C.

In a conventional piston type damper, C_d is a function of the flow rate of a damping fluid from one side of a piston to the other. When the orifice through which the fluid must pass is small, a large pressure drop through it occurs, resulting in a pressure differential across the piston. When this pressure differential is multiplied by the area of the piston, a force results in a direction to oppose the motion of the piston. For large orifice area, the pressure drop is small, thus the force is small and a low damping coefficient results. Conversely, for a small orifice area the force is large and a large damping coefficient results. For a more complete treatment see (10).

This investigation is a study of a nonlinear damper for vibration isolation utilizing the theory of damping coefficient control stated above. To accomplish this, an electronic analog (Fig. 2-5) was constructed and the performance compared to that predicted by the theory. A design proposal for the mechanical model is also presented.

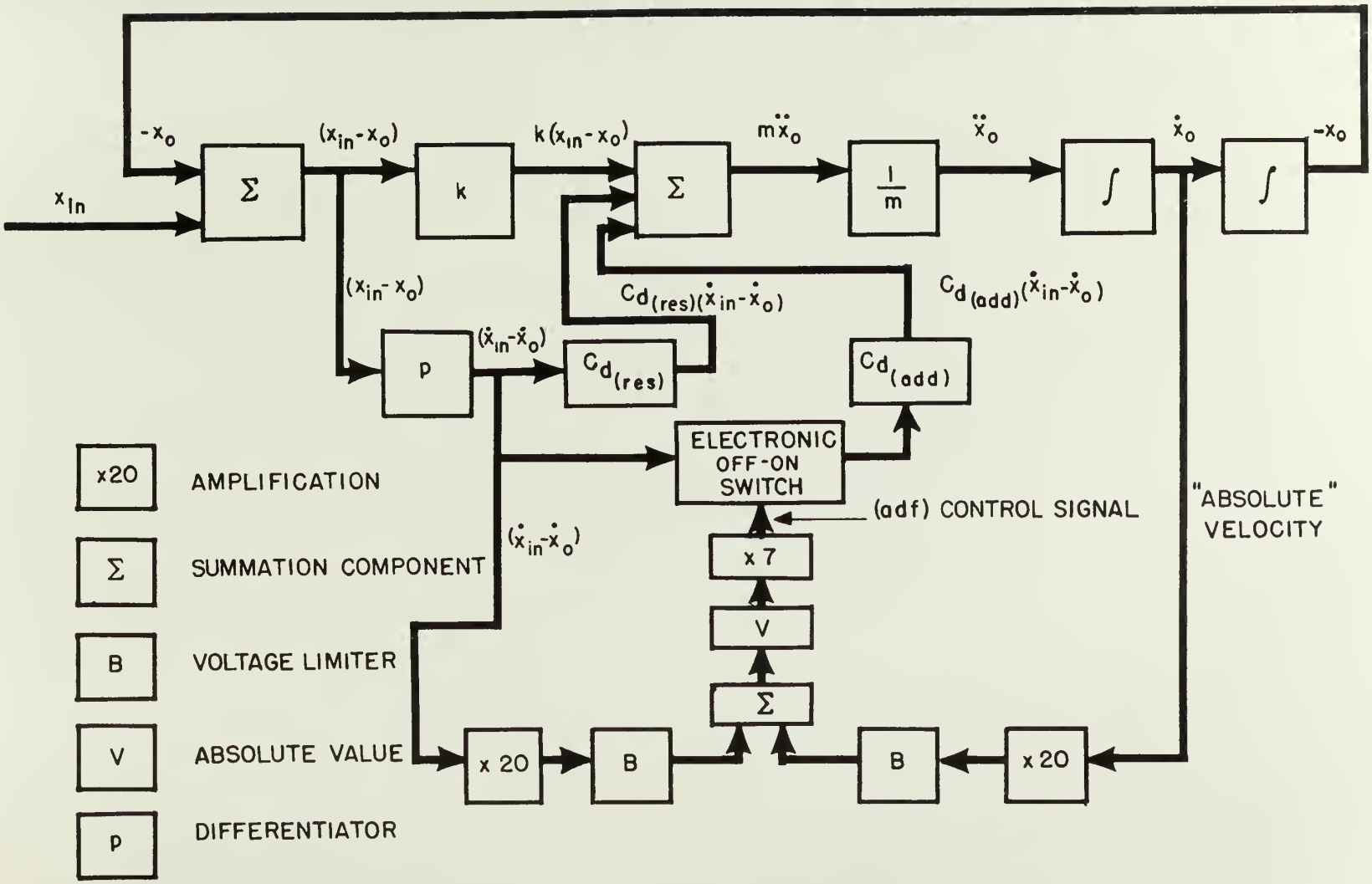

Fig. 2-5 Electronic Analog of a Second Order System with Ideal Damping

CHAPTER 3

DESCRIPTION OF EQUIPMENT

In the study of an ideal vibration damper, a second-order system with a controllable damping coefficient was constructed by use of the George A. Philbrick Researches, Inc. (GAP/R) high-speed, all-electronic, analog computer. The unit consists of self-contained components each designed to accomplish specific operations.

The computer components used in this study are listed below.

(1) K3-A Adding Component
(2) K3-C Coefficient Component (Amplifier)
(3) K3-J Integrating Component
(4) K3-D Differentiating Component
(5) K3-B Bounding Component. The function of this component is to transmit the input signal to the output except when the input excursion exceeds certain selected positive or negative values. The magnitude of the output is thus limited to these selected values.
(6) K3-V Absolute Value Component. The function of this component is to receive a plus or minus input signal and to rectify this signal for the output.

In addition to the above listed components, a Central Component, Model CC, was used to obtain a delta wave input to the system in order to obtain transient response. The delta wave is made up of four approximately equal intervals with a neutral at zero and an adjustable positive and negative output.

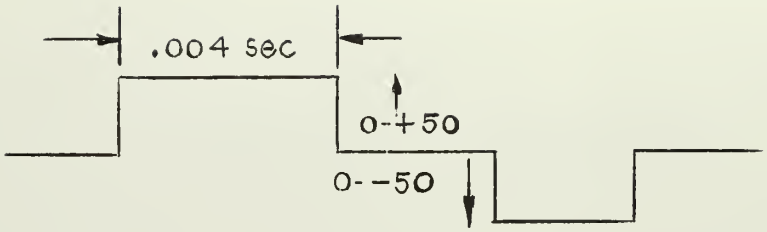

This provides a plus and a minus step input with zero initial condition.

The Model RS, Regulated Power Supply, was also utilized to give a closely-regulated power supply for the operational components.

For a further description of the above-listed units, see (11).

A General Radio Co. Beat Frequency Oscillator was used to provide a sinusoidal input to the system to obtain frequency response data.

Results were displayed on a type 304-HR Cathode Ray Oscilloscope manufactured by the Allen B. Dumont Laboratories, Inc. The output of the CRO was recorded photographically by a Polaroid Oscillograph-Record Camera also provided by the Allen B. Dumont Laboratories.

CHAPTER 4

INVESTIGATION

4.1 Electronic Analog

In order to simulate the ideal damper performance on an electronic analog computer, an ordinary second-order system was set up based on Eq. (2-1).

$$- m\ddot{x}_o + C_d(\dot{x}_{in} - \dot{x}_o) + k(x_{in} - x_o) = 0$$

The first attempt was to utilize a set-up using integrators only. The operator form of Eq. (2-1) is:

$$x_o = \left[\frac{C_d p + k}{m p^2 + C_d p + k}\right] x_{in}$$

or by rearranging:

$$x_o = \left[\frac{x_{in}}{m p^2 + C_d p + k}\right] (C_d p + k)$$

$$= x'_o (C_d p + k)$$

From this,

$$x'_o = \frac{x_{in}}{m p^2 + C_d p + k}$$

or in the time domain

$$m\ddot{x}'_o = x_{in} - C_d\dot{x}'_o - kx'_o$$

Then:

$$\ddot{x}'_o = (1/m)m\ddot{x}'_o$$

$$\dot{x}'_o = \int \ddot{x}'_o\,dt$$

$$x'_o = \int \dot{x}'_o\,dt$$

This resulted in a set-up as follows:

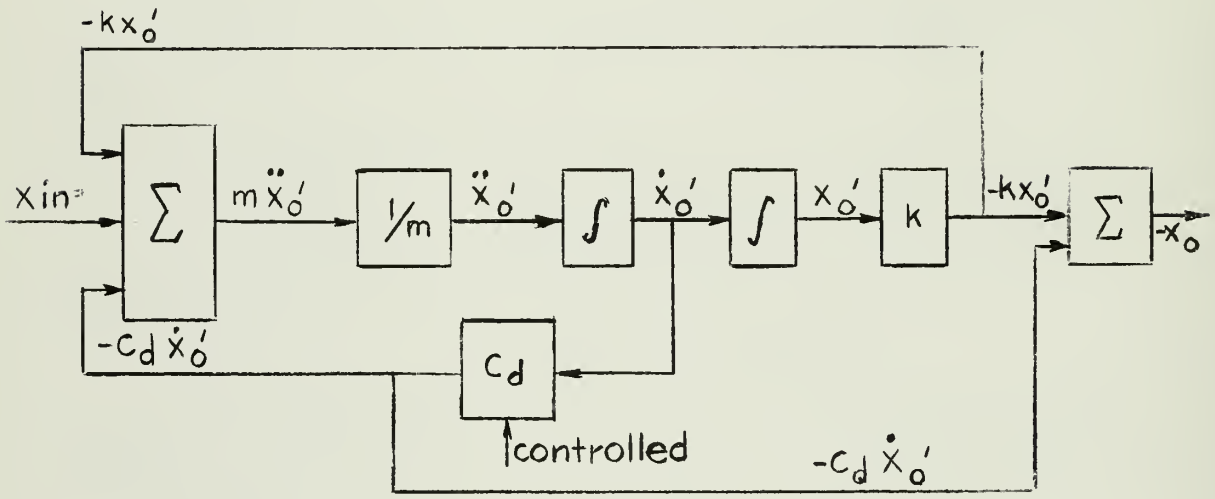

Unsatisfactory data led to rechecking the system. It was found that this set-up is satisfactory for linear systems where only x_{in} is varied, i.e., the resulting kx'_o remained properly phased with $C_d\dot{x}'_o$; but with a nonlinearity introduced on $\dot{x}'_o$ by the C_d amplifier, the phasing of kx'_o did not correspond to that of $C_d\dot{x}'_o$ due to the location in the loop of the integrations. The resulting x_o was not correct, and a true comparison of $\dot{x}_o$ with $\dot{x}_{in}$ was not obtained.

It was therefore found necessary to introduce the nonlinearity directly on $(\dot{x}_{in} - \dot{x}_o)$. This required using a differentiator and

the set-up used is as shown in Fig. 2-5. The results were satisfactory.

An electronic switch (See Appendix A) was incorporated to act as an "on - off" control for $C_{d(add)}$, utilizing the control criterion previously established.

To provide a control signal for the switch, the relative velocity ($\dot{x}_{in} - \dot{x}_o$) voltage was amplified and then limited to two volts. This signal was then subtracted from the "absolute" velocity ($\dot{x}_o$) signal which was also amplified by the same amount and limited to two volts. The result was a plus or minus four volts when the velocities were of opposite sign and a zero voltage where they were of the same sign. Since the signs of the velocities are the real criterion for control, the amplification provides a definite and more rapid indication when a change in sign occurs. The limiting provides that the results of the comparison be definite voltages representing the algebraic signs of the velocities.

The $C_{d(add)}$ is desired in the system during the interval when the velocities are of opposite sign. At this time the output of the computer component where the subtraction is performed is a plus or minus four volts. The electronic switch is biased to be actuated by a positive signal of at least 20 volts, thus the absolute value of the velocity comparison signal is amplified and becomes the additional-damping-force (adf) control signal. This signal turns the switch "on" which effectively introduces $C_{d(add)}$ into the system. When the (adf) signal becomes zero, the switch returns to its "off" position and only the $C_{d(res)}$ is left to provide the damping force. When one of the velocity signals is zero, a two-volt signal results. This is an instantaneous condition, however, and will not affect the operation of the switch.

Fig. 4-6 shows a sequence of steps undergone by the velocities to produce the (adf) control signal for a step input.

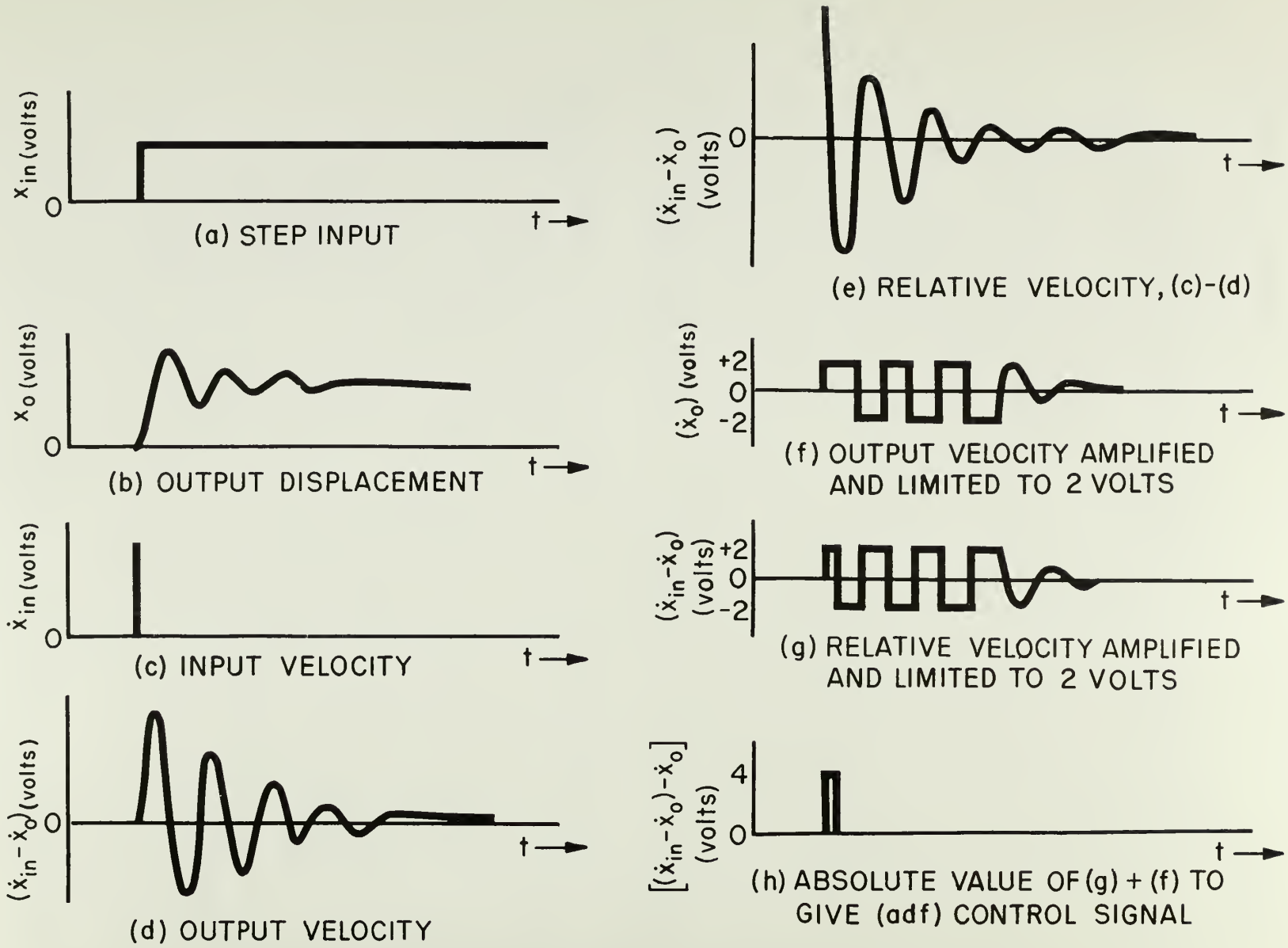

Fig. 4-6 Typical Theoretical Relationships of Absolute and Relative Velocities in Obtaining the (adf) Control Signal for a Step Input

Figure 4-7 shows a comparison of typical velocities to produce the (adf) control signal for a sinusoidal input.

Transient response of the system was obtained by introducing a step input voltage to the system and recording the output displacement, displayed on a Cathode Ray Oscilloscope, with a Polaroid camera.

Frequency response was obtained by using a sinusoidal voltage input and recording the output in a similar manner to the transient response. Three runs were made using different values of the parameters k, m, $\zeta_{(res)}$, and $\zeta_{(add)}$.

Difficulties were encountered in obtaining transient response data in that the balance of the diode bridge in the switch was not perfect and the relative velocity signal was affected by components of the (adf) control signal.

The following is a tabulation of the parameters used in obtaining the frequency and transient response data.

TRANSIENT RESPONSE

Run	k (lb/ft)	m (slugs)	$\zeta_{(res)}$	$\zeta_{(add)}$	W_n (rad/sec)
1	0.95	1	0.165	1.3	0.975
2	1.0	1	0.072	2.15	1.0
3	0.478	1	0.118	0.667	0.68

FREQUENCY RESPONSE

4	30	1	0.112	1.12	5.49
5	60	1	0.14	1.57	7.75
6	120	1	0.121	2.07	11.0

In obtaining the frequency response, much difficulty was encountered due to drift of the computer components. It was necessary to allow the computer to warm up for at least one hour

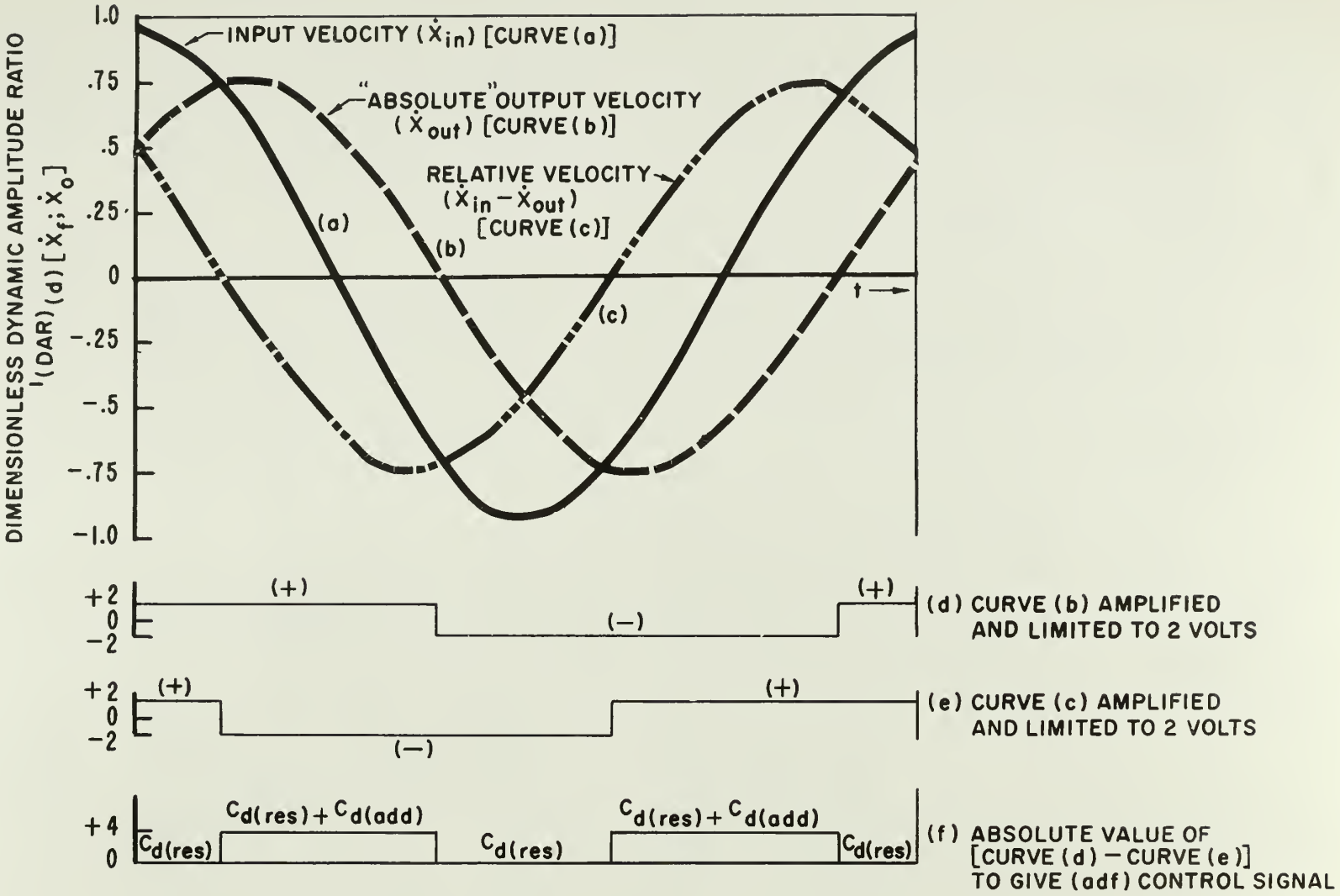

Fig. 4-7 Typical Theoretical Relationships of Absolute and Relative Velocities in Obtaining the (adf) Control Signal for a Sinusoidal Input

before the drift could be reduced to a point where even qualitative data could be obtained. The (adf) control signal was extremely sensitive to drift and frequent readjustments of that circuit were necessary to maintain the desired control of $C_{d(add)}$ Collection of the frequency response data was therefore a long and tedious process.

4.2 Design of an Experimental Model

It has been previously stated that the damping coefficient can be controlled by varying the orifice area through which the damping fluid must pass. This fact was utilized in the design of the experimental model.

The method proposed by Professor Li to accomplish this consists of two sleeves mounted concentrically on the damper piston but which can move independently through a limited travel with respect to the piston (Fig. 4-8). Ports are drilled in the two sleeves and in the piston itself such that when the sleeves are positioned at opposite extreme ends of their travel, the ports are aligned and maximum orifice area exists resulting in a low damping coefficient. When the sleeves are positioned at the same ends of their extreme travel, the orifice area is reduced to zero and the only flow allowed is that through the small clearances between the piston, sleeves, and cylinder. This condition represents a high damping coefficient. Thus by design, the maximum orifice opening corresponds to $C_{d(res)}$ and zero orifice opening corresponds to $C_{d(res)} + C_{d(add)}$.

Each sleeve is controlled independently. The outer sleeve, "A" in Fig. 4-8, is sensitive only to relative motion between the cylinder and piston. The cylinder represents the input velocity and the piston represents the output velocity. Three forces act on this outer sleeve, one being the viscous shear force between the cylinder wall and the sleeve which is opposed by a second viscous shear force between the sleeve and the piston. This

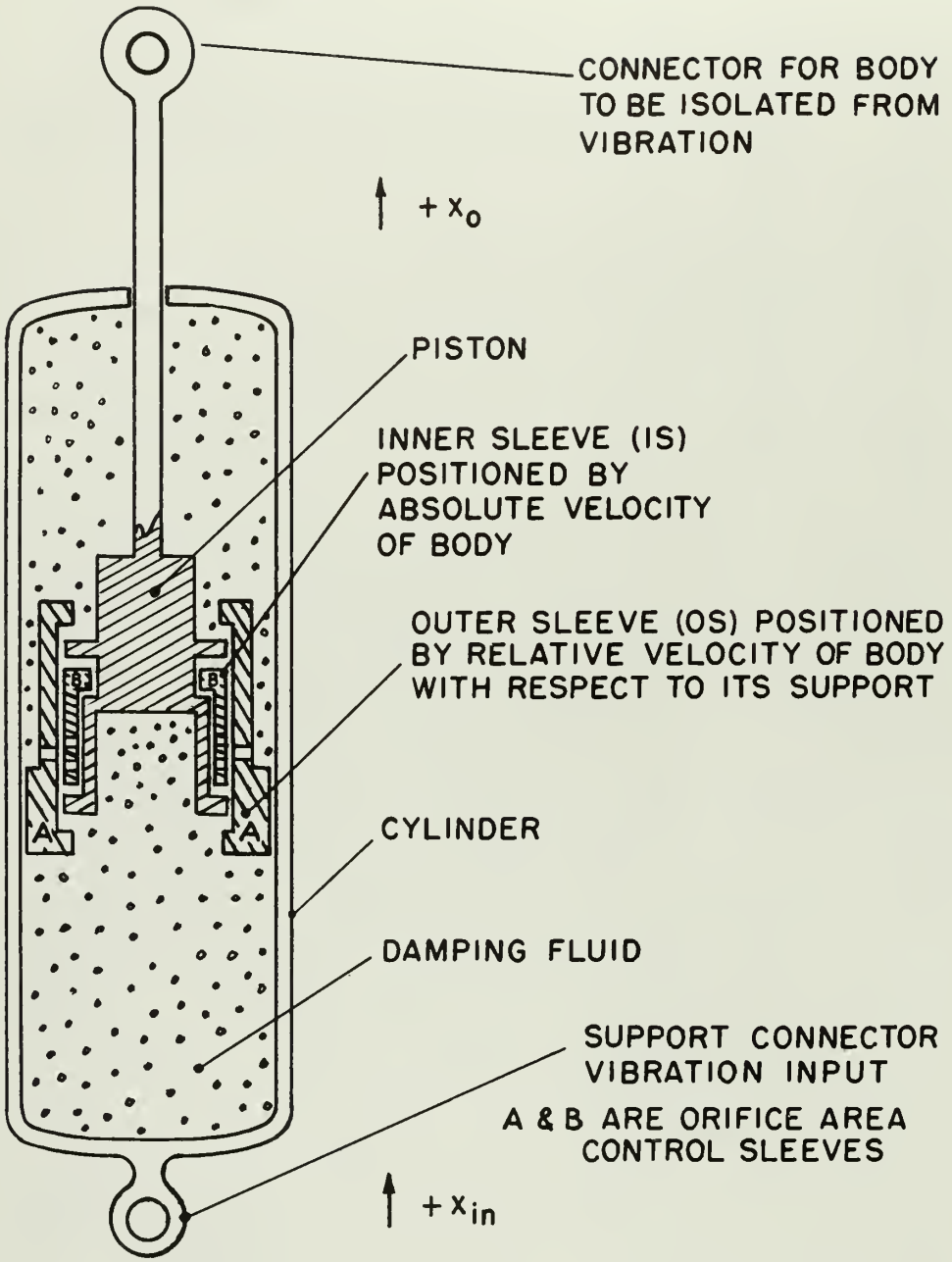

Fig. 4-8 Schematic Diagram of Ideal Damper

second force is small, thus the resultant tends to position the sleeve at either of its extreme positions depending on the direction of the relative velocity. The third force is due to a pressure differential force across the sleeve, created again by the relative velocity, which aids the resultant viscous force in positioning the sleeve.

The inner sleeve is designed basically as a velocimeter and is sensitive only to the "absolute" velocity of the piston. It is positioned at either of its extreme limits by this velocity.

By the positioning of the two sleeves, the desired control of the damping force is realized. The damping force control criterion is summarized below.

Output Velocity $\dot{x}_o$	Position of (is) with respect to piston	Relative Velocity $\dot{x}_r = (\dot{x}_m - \dot{x}_o)$	Position of (os) with respect to piston	Orifice	Damping Force $C_d \dot{x}_r$	C_d
+	Down	+	Up	Closed	Desirable	$C_{d(res} + C_{d(add)}$
-	Up	+	Up	Open	Adverse	$C_{d(res)}$
+	Down	-	Down	Open	Adverse	$C_{d(res)}$
-	Up	-	Down	Closed	Desirable	$C_{d(res} + C_{d(add)}$

Fig. 4-9 presents a schematic drawing of the piston in cross-section showing the four possible extreme positions of the two sleeves with respect to the piston. Fig. 4-9(a) and (d) show the positions of the sleeves to obtain the desired high damping coefficient when the velocities are of opposite sign. Fig. 4-9(b) and (c) show the positions of the sleeves to obtain a low C_d for the velocities having the same signs.

Fig. 4-10 is the exploded-view of the experimental model which includes an amplification stage. The amplification stage is presented schematically in Fig. 4-11. The need for the amplification becomes apparent when the requirements of the (adf)

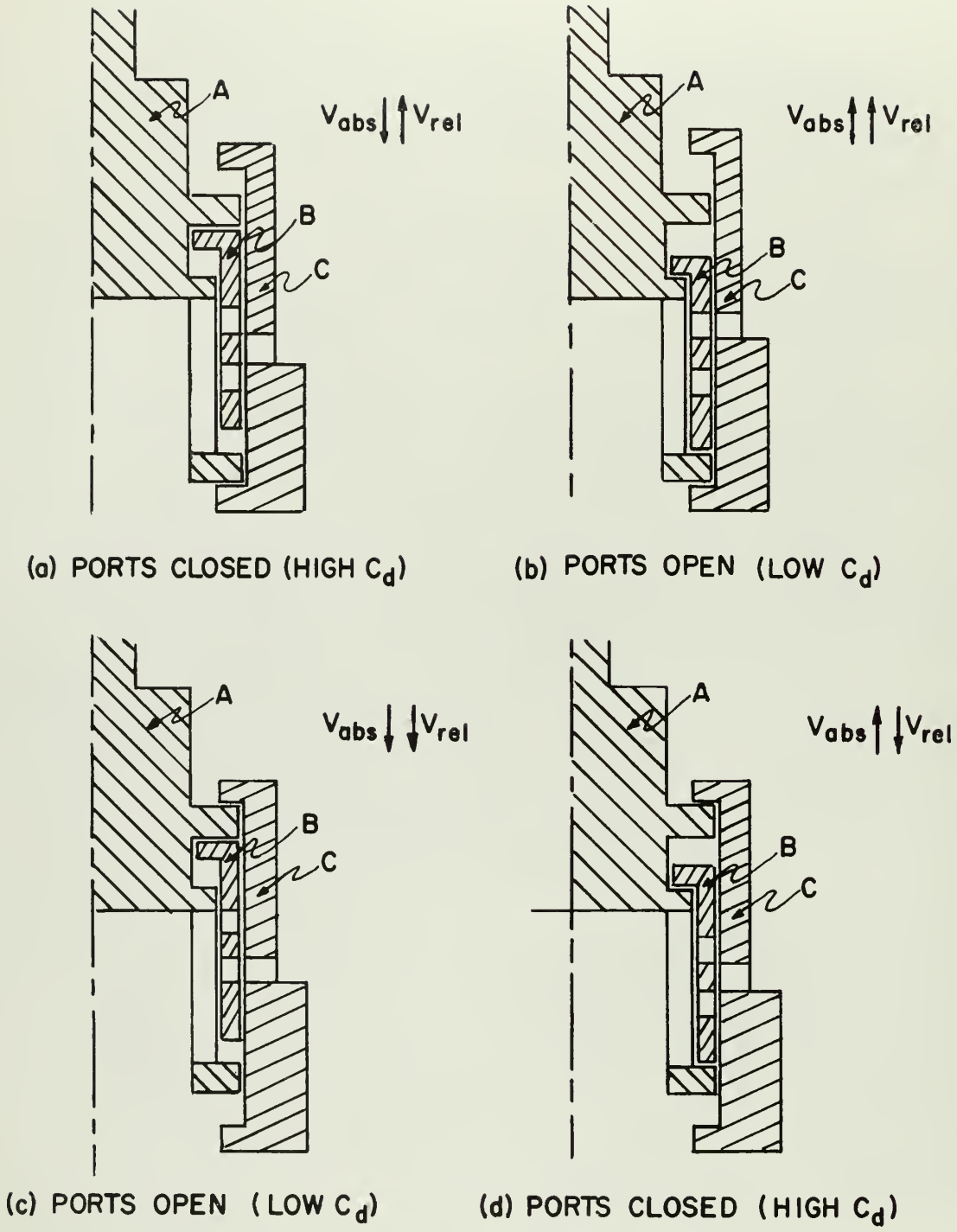

Fig. 4-9 Cross-Sectional View of Piston of Ideal Damper Showing the Four Relative Positions of the Sleeves

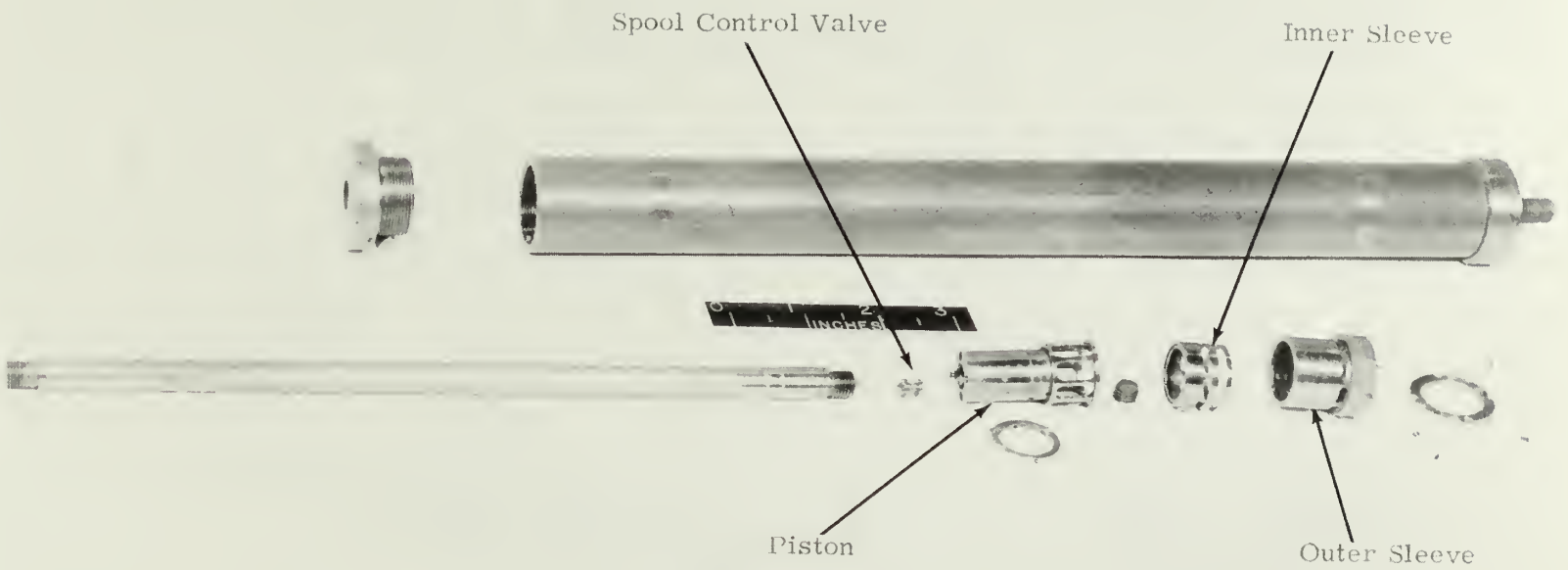

Fig. 4-10 Experimental Model of Ideal Damper

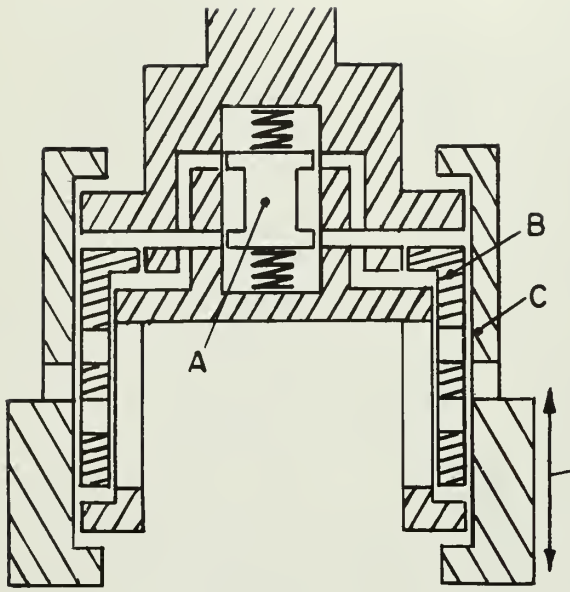

a) CROSS-SECTION OF PISTON SHOWING SPOOL CONTROL VALVE (A). (SPOOL IS ALSO THE SEISMIC MASS IN THE VELOCIMETER.) FIGURE ALSO SHOWS "UP" AND "DOWN" PORTS WHICH CONTROL POSITION OF THE INNER SLEEVE (B).

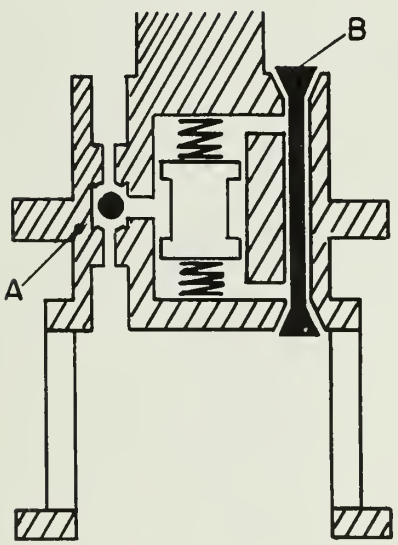

b) CROSS-SECTION OF PISTON. BALL CHECK VALVE (A) SELECTS HIGH PRESSURE SIDE OF PISTON. THE SPINDLE VALVE SELECTS THE OPPOSITE OR LOW PRESSURE SIDE OF PISTON TO PROVIDE EXHAUST PASSAGE.

Fig. 4-11 Cross-Sectional View of the Ideal Damper Piston, Sleeves, and Spool Control Valve

control valve, consisting of the inner and outer sleeves, are considered. Since the (adf) control criteria is based on the algebraic signs of the "absolute" and relative velocities, the sensitivity of the control must be very high. The relative velocity sensing device (outer sleeve) fulfills this requirement, but the "absolute" velocity device (inner sleeve) without the amplification does not.

The displacement of the inner sleeve without amplification would be proportional to the magnitude of absolute velocity, giving only a small displacement for a small velocity. It is desired, however, that this sleeve be positioned at the limit of its travel by this small velocity signal, thus fully opening or closing the valve port. For this reason, the sensitivity of the valve must be increased by the amplification stage. Another required condition is that the valve must not overshoot to keep the valve port open or closed as the case may be. For this reason a stop at each end of the travel, together with a high sensitivity, is necessary to operate the valve. However, from the standpoint of the velocimeter operation, a stop is undesirable. For example, if the input velocity should be of an amplitude to position the sleeve against its stop, a further increase in velocity would not be sensed, thus any subsequent decrease in velocity would take the sleeve off its stop prematurely and give the wrong value for C_d. The spool valve in the amplification stage must be designed so that it will not hit its stops within a reasonable velocity range

The amplification stage consists of a seismographic system designed to operate in the velocimeter range (Fig. 4-11(a)). The seismic mass is positioned statically by two very soft springs. The dynamic position of the seismic element responds to the input velocity, opening a port in such a manner as to allow a pressure force to be applied to the inner sleeve. This force positions the sleeve at either of its extreme limits of travel corresponding to the direction of the displacement of the seismic mass. The pressure on the opposite side of the sleeve

is relieved to exhaust by the seismic element position also. Opposite displacement of the seismic element causes the sleeve to be positioned at its opposite stop.

Supply pressure is obtained by a ball check valve selecting the high pressure side of the damper piston, and exhaust is achieved by a spindle valve selecting the low pressure side of the piston (Fig. 4-11(b)).

In order to achieve linear operation of a velocimeter, the relative displacement amplitude must have a constant, or near constant, ratio to the forcing velocity amplitude and a dynamic response angle of, or near, 180^{o}. The linear range of a velocimeter is greatest for high values of damping ratio but the sensitivity is small. Since the sensitivity of the velocimeter can be low and still accomplish the desired amplification, the damping ratio can be high and thus provide a wide band width.

Appendix B presents a development of the performance functions for the displacement of the inner sleeve corresponding to a velocity input. Appendix B also includes the actual design criteria for the velocimeter resulting in the following parameters for the spool valve.

$$\zeta = 103$$

$$W_n = 8 \text{ rad/sec}$$

$$k = 0.1 \text{ gm/cm}$$

$$m = 1 \text{ gm}$$

CHAPTER 5

CONCLUSIONS AND RECOMMENDATIONS

In order to verify the predicted performance of the nonlinear damper proposed by Dr. Li, an electronic analog for a second-order system for vibration isolation, including the nonlinear damping term, was constructed and tested.

Fig. 5-12 shows oscillographic recordings of the output of the system for a step voltage input corresponding to a step displacement input. Fig. 5-12(a) shows the step input. Fig. 5-12(b) shows the displacement output for low damping ($C_d = C_{d(res)}$), and Fig. 5-12(c) shows the output for high damping ($C_d = C_{d(res)} + C_{d(add)}$). Fig. 5-12(d) shows the output of the system for nonlinear damping. Initially, the curve has the same slope as the low damped curve, but then the $C_{d(add)}$ is introduced and the resulting curve approaches its final value gradually and smoothly. This is a desired ideal performance of the nonlinear damper. Perfect damping is approached in that little or no shock load is transmitted to the body and no oscillations result. Heretofore this has not been realizable damper performance. Fig. 5-12(e) shows a comparison of 5-12(b), (c), and (d).

Figure 5-13 shows the relative velocity signals on which the damping is based. Figs. 5-13(a) and (b) show relative velocity for low and high damping respectively, and Fig. 5-13(c) shows the velocity signal as modified by the nonlinearity in the system. Fig. 5-13(d) shows the (adf) control signal which introduced $C_{d(add)}$ after the input velocity went to zero.

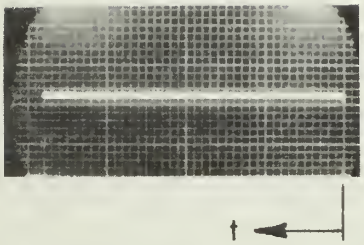

(a) STEP INPUT

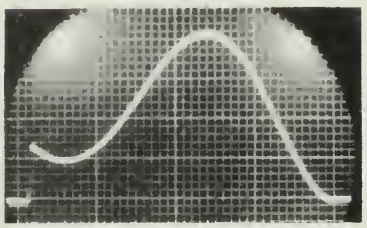

(b) OUTPUT OF LOW DAMPED SYSTEM
$C_d = C_{d_{(res)}}$

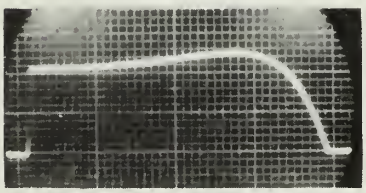

(c) OUTPUT OF HIGH DAMPED SYSTEM
$C_d = C_{d_{(res)}} + C_{d_{(add)}}$

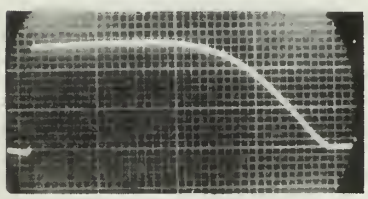

(d) OUTPUT OF IDEALLY DAMPED SYSTEM
$C_d = C_{d_{(res)}} + C_{d_{(add)(CONTROLLED)}}$

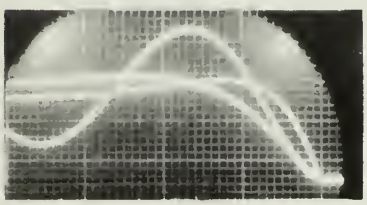

(e) OUTPUTS OF SYSTEM WITH LOW, HIGH, AND IDEAL DAMPING

Fig. 5-12 Transient Response Amplitude Ratios; Run 3

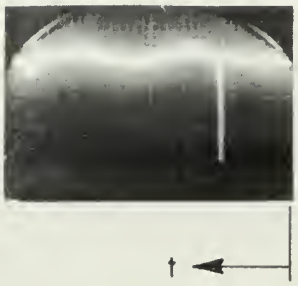

(a) RELATIVE VELOCITY, LOW DAMPED SYSTEM OF FIG. 12(b).

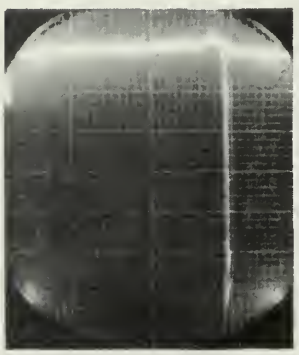

(b) RELATIVE VELOCITY, HIGH DAMPED SYSTEM OF FIG. 12(c).

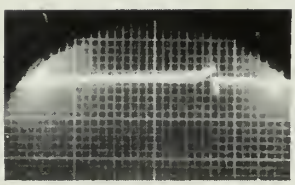

(c) RELATIVE VELOCITY OF FIG. 12 (d) WITH IDEAL DAMPING.

(d) ADDITIONAL DAMPING FORCE (adf) CONTROL SIGNAL OF FIG. 12 (d)

Fig. 5-13 Relative Velocities and (adf) Control Signal of Fig. 5-12

Three runs for transient response were made for the different parameters listed in Chapter 4, however, only oscillographs for one run are included here because the results were practically identical. It will be noted that the transient response for the nonlinear damper represents considerable improvement over the "Inertial Controlled" damper response presented in Fig. 1-2.

Fig. 5-14 shows a typical response of the system for a sinusoidal input. Fig. 5-14(a) shows the sinusoidal input while Figs. 5-14(b) and (c) show the outputs for low and high damping respectively. Fig. 5-14(d) shows the output for ideal damping. It is noted that distortion of the output occurs, but the amplitude ratio is less for the nonlinear system than for either the high or low damping ratio. These oscillographs were for Run 6 at a frequency ratio of 1.3. Fig. 5-15 shows the relative velocities and (adf) control signal for Run 6.

Figs. 5-16, 17, and 18 show the complete nondimensionalized frequency response of the system for high, low, and nonlinear damping for Runs 4, 5, and 6 respectively. Each run was for a different set of parameters as listed in Chapter 4. It will be observed that in all three curves, the performance of the system with nonlinear damping is superior to that of either low or high damping in the natural frequency region. At low frequency ratios the nonlinear damper maintains an amplitude ratio of unity over a greater bandwidth than either the high or low damped cases. It then decreases to an amplitude ratio below that of the other two. For all other frequencies the amplitude ratio for the nonlinear system is considerably lower than for the high damped system. It is lower also than the low damped system up to a frequency ratio of 2.5 for Runs 1 and 3 and 1.7 for Run 2. Beyond this point the amplitude ratio of the low damped system is lower. This is acceptable performance since the amplitude ratio is very low at these frequencies.

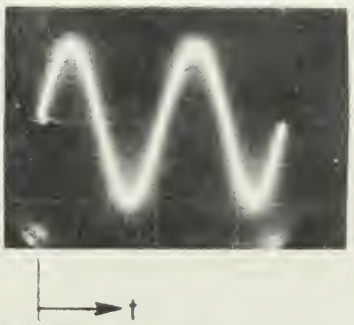

(a) INPUT

t

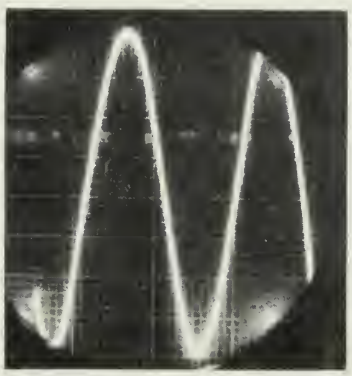

(b) OUTPUT OF LOW DAMPED SYSTEM $C_d = C_{d_{(res)}}$

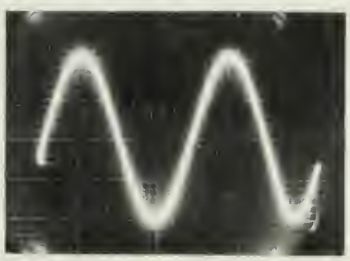

(c) OUTPUT OF HIGH DAMPED SYSTEM $C_d = C_{d_{(res)}} + C_{d_{(add)}}$

(d) OUTPUT OF IDEALLY DAMPED SYSTEM $C_d = C_{d_{(res)}} + C_{d_{(add)}}$ (CONTROLLED)

Fig. 5-14 Frequency Response Amplitude Ratios at β = 1.3; Run 6

(a) RELATIVE VELOCITY

t

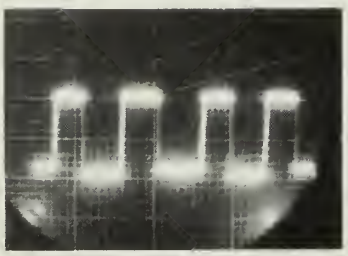

(b) ADDITIONAL DAMPING FORCE (adf) CONTROL SIGNAL

(c) MODIFIED RELATIVE VELOCITY

Fig. 5-15 Relative Velocities and (adf) Control Signal of Fig. 5-14

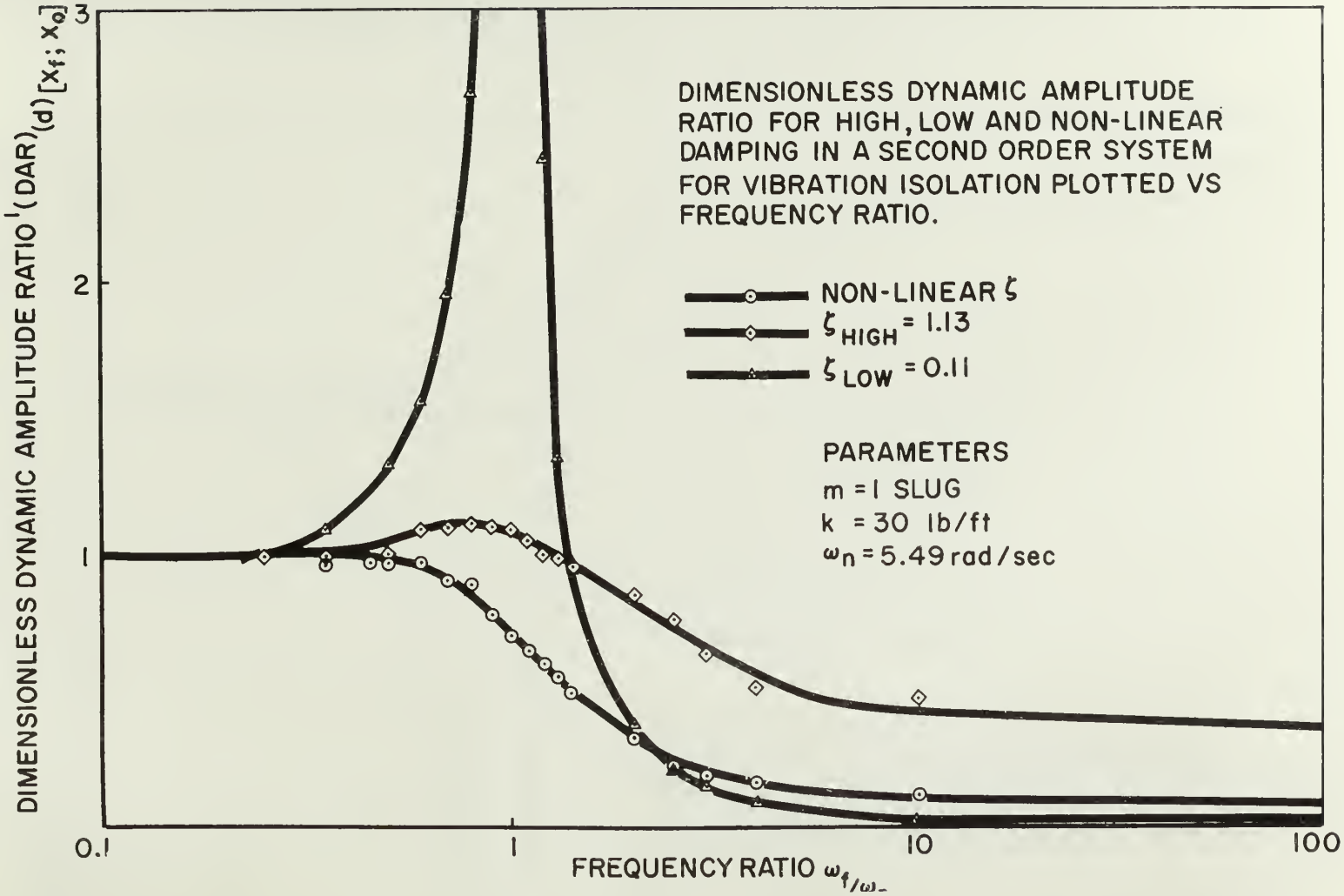

Fig. 5-16 Frequency Response Amplitude Ratios; Run 4

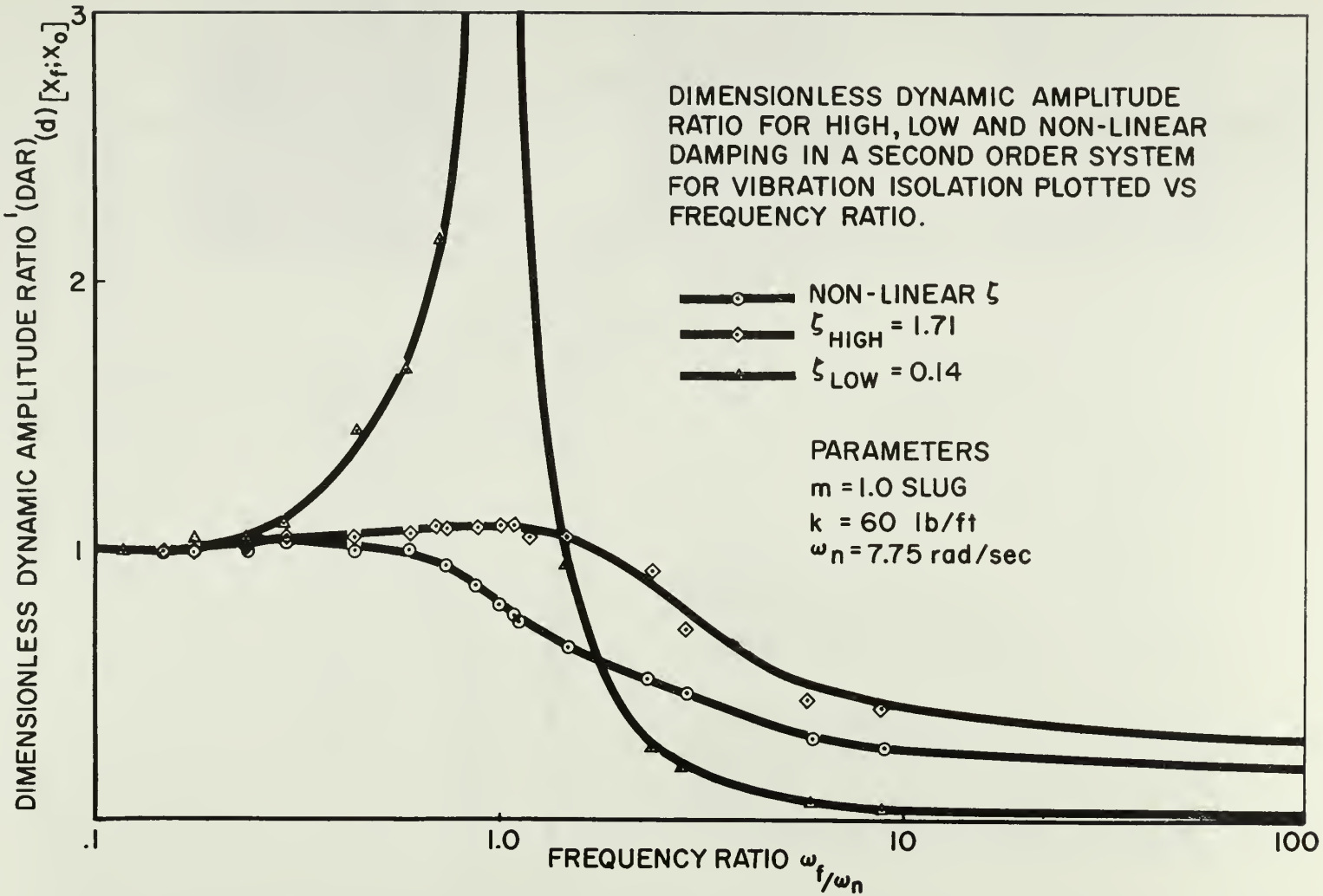

Fig. 5-17 Frequency Response Amplitude Ratios; Run 5

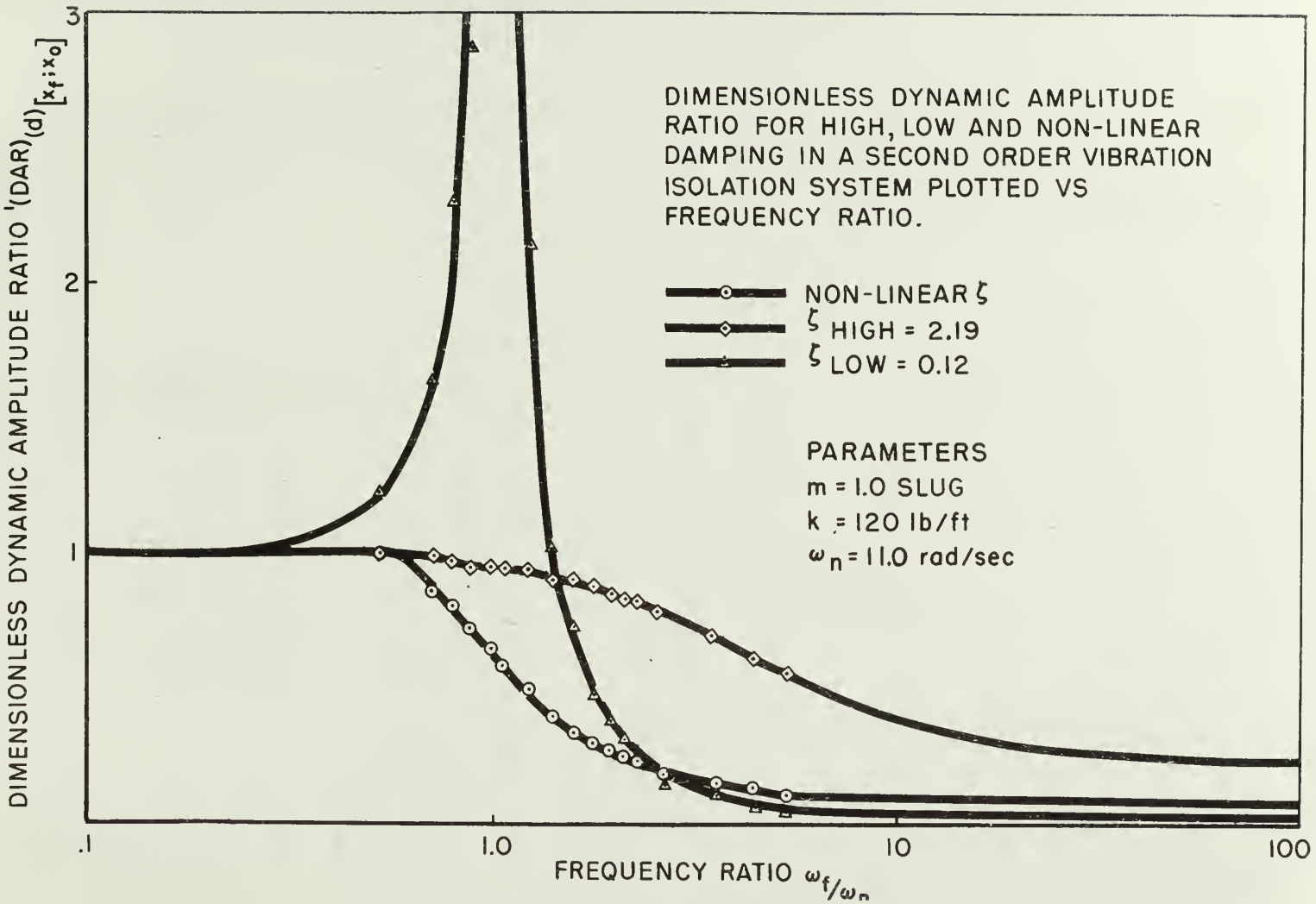

Fig. 5-18 Frequency Response Amplitude Ratios; Run 6

In Fig. 5-19 the results for the three runs are plotted together. It will be noted that good correlations exist. The differences are accounted for by the change in parameters, the possible nonlinearity of the input signal, and the fact that amplifier drift was ever present in the system causing the control of $C_{d(add)}$ to be other than desired except for those times immediately following its precise adjustment.

Fig. 5-20 shows a comparison of the nonlinear damper performance to the perfect damper performance as previously described, and to the optimum performance of the "frequency-selective" damper proposed in (6). It will be noted that performance of the nonlinear damper is equal to or superior to that of the frequency selective class at all except high frequencies where the performance for both systems is comparable.

Fig. 5-21 presents a comparison of the system with nonlinear damping compared to a conventional system with high and low damping and to the perfectly damped system with damping ratio of 0.85.

In the transient response it was noted that a small phase difference occurred between the (adf) control signal and the output displacement. It is recommended that lead-lag components be inserted in the system to compensate, thus improving the transient response.

Drift was the major problem in the frequency response. It is therefore recommended that all computer components be stabilized. This would result in more quantitative results in that it was difficult to obtain accurate data when the output signal was drifting

The "dead-zone" in the electronic switch could be narrowed by a redesign, thus improving its control of the damping

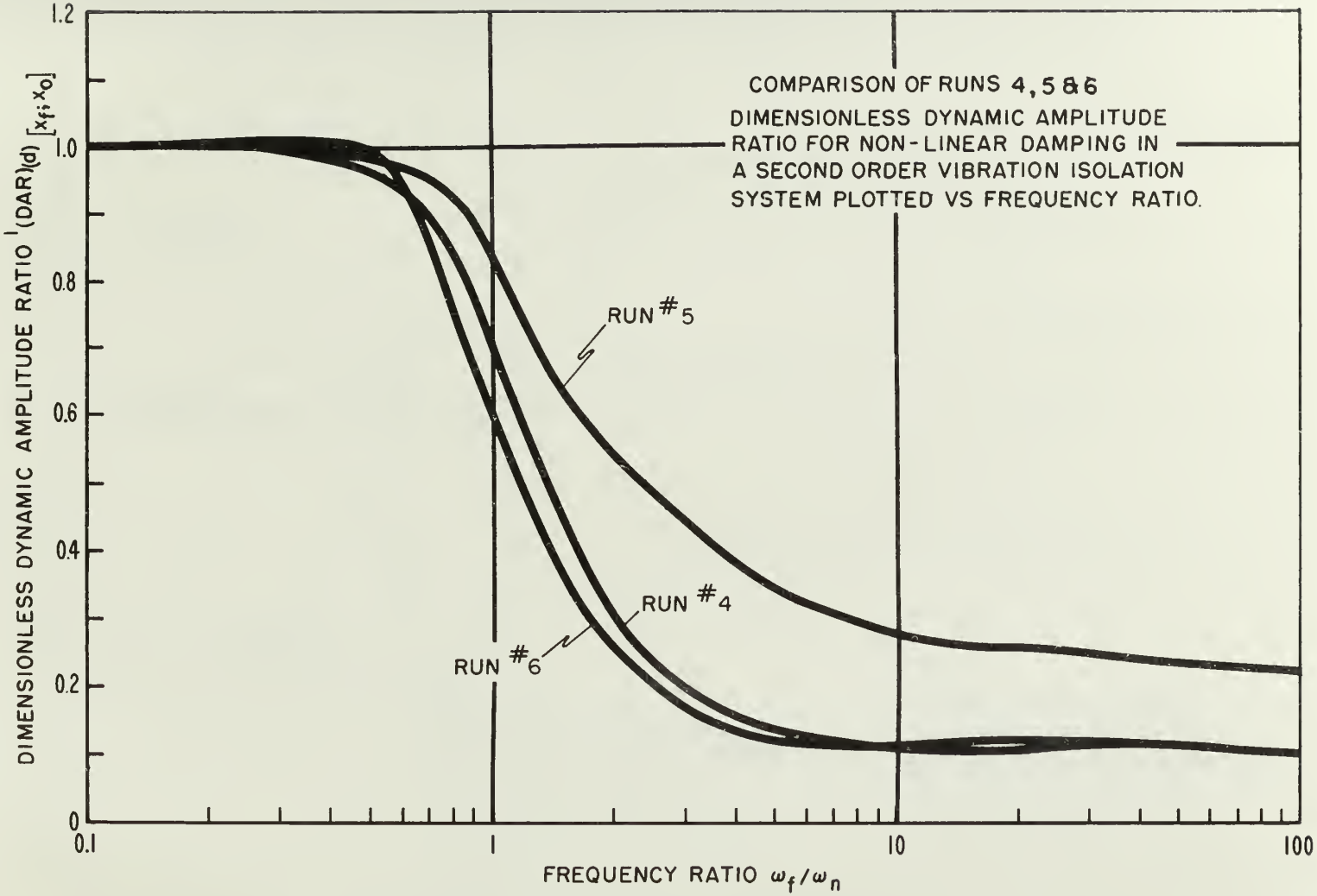

Fig. 5-19 Frequency mplitude Ratios of Runs 4, 5, and 6, with Nonlinear Ideal Damping

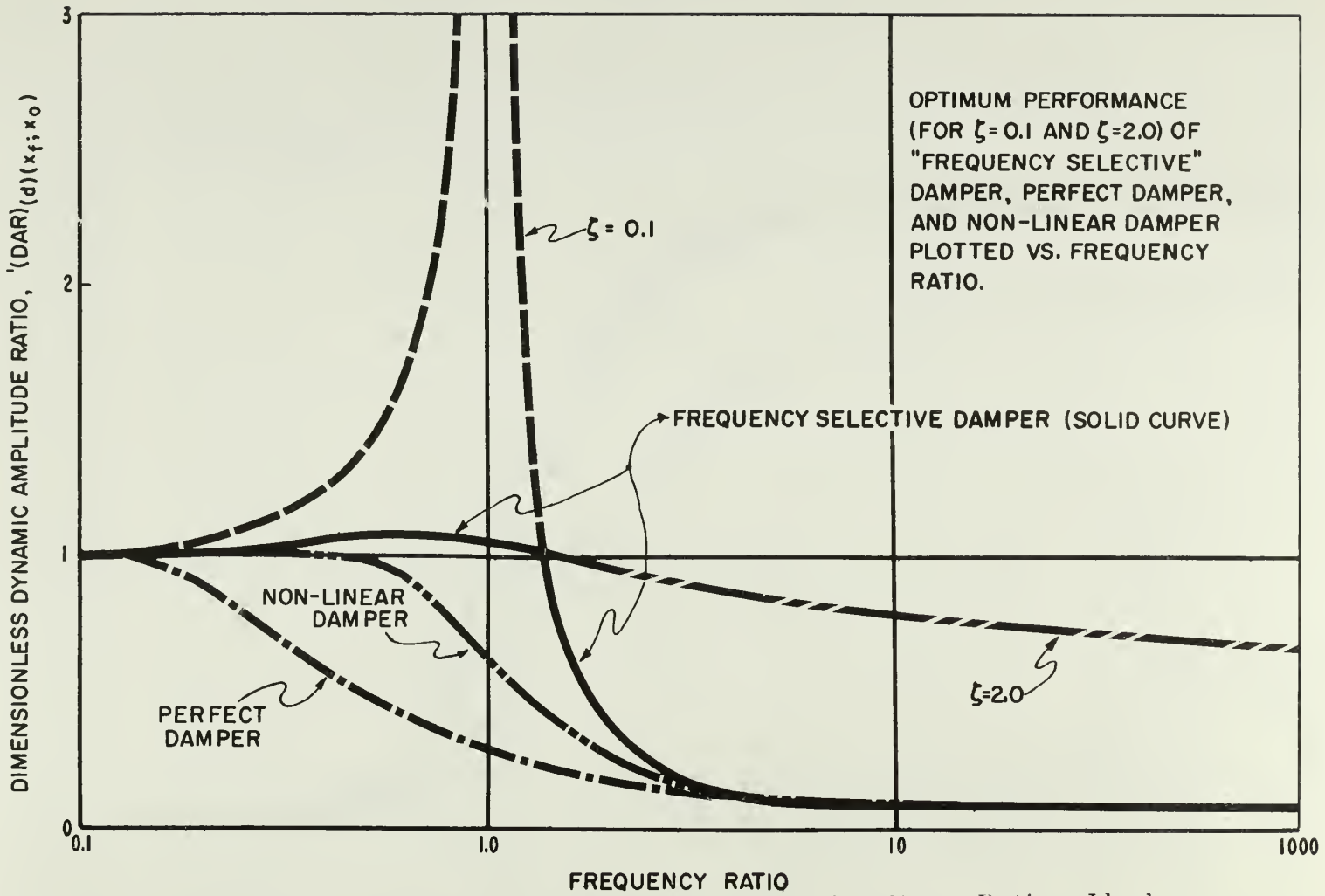

Fig. 5-20 Typical Frequency Response Amplitude Ratios; Ideal Damping, Optimum "Frequency-Selective" Damping, and Perfect Damping

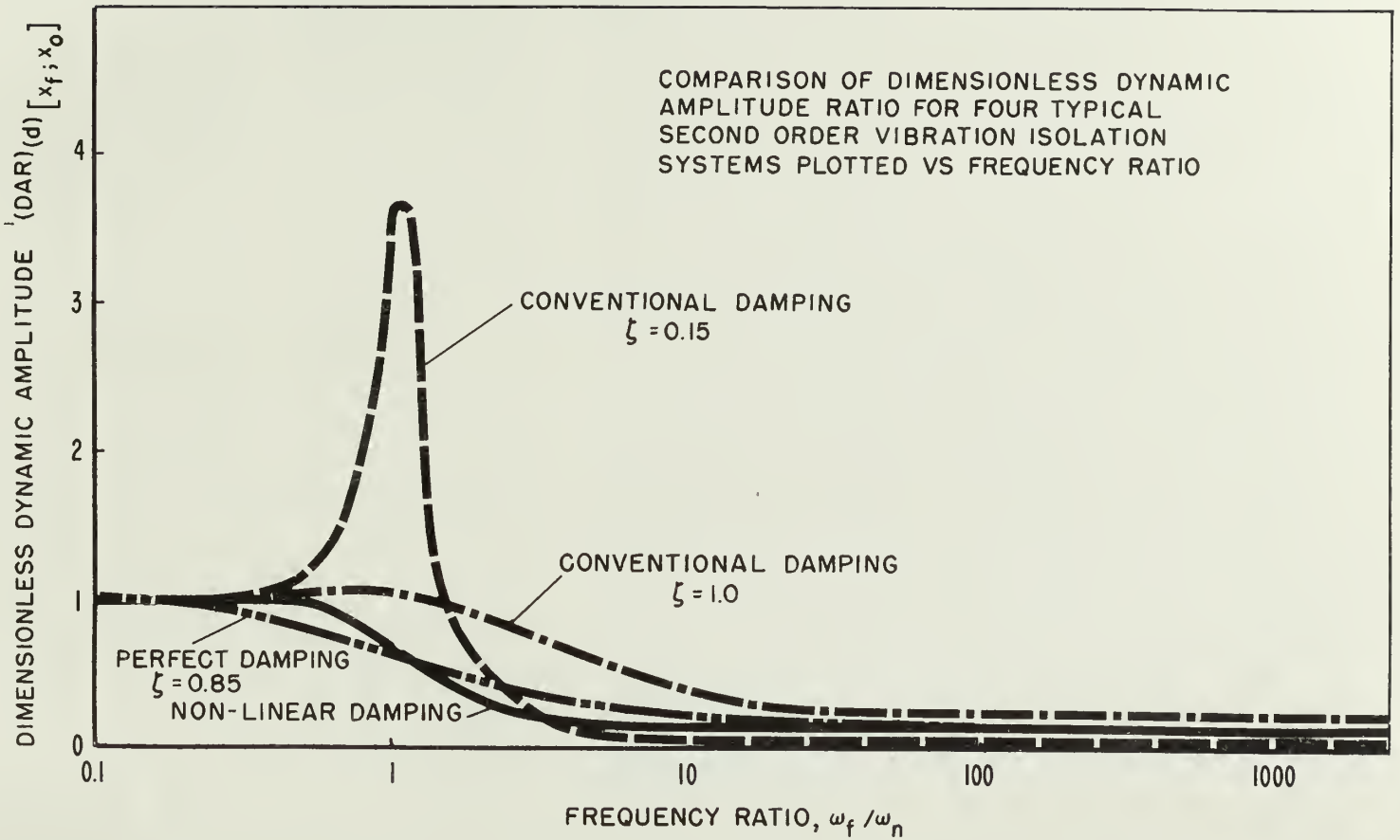

Fig. 5-21 Typical Frequency Response Amplitude Ratios; Ideal Damping, Conventional Damping, and Perfect Damping

coefficient. It is also recommended that the electronic switch not be used to pass the velocity signal but rather to act as a short-to-ground switch to eliminate $C_{d(add)}$ when it is not required. This would eliminate any effect of a distortion that the signal would pick up when passing through the switch.

For obtaining the frequency response, it is felt that if the quality of the amplification of the velocities (especially relative velocity which is very small at low frequencies) for the (adf) was increased, a more positive control of $C_{d(add)}$ could be obtained. At low frequencies the results would then more closely approach those of the perfect damper.

At higher frequencies where the relative velocity is larger, the indicated performance could be improved if the necessary high amplification of the (adf) control velocities was decreased. Decreasing the amplification below saturation of the amplifiers in the (adf) control circuit would eliminate the delay associated with the unstabilized amplifiers returning from saturation. The frequency whose period approaches this delay time was a limit for frequency response.

It is recommended that tests be performed on the experimental model presented in Fig. 4-10. It is further recommended that these tests be conducted on a vertical shaper available at the Institute. This shaper provides a forcing frequency and amplitude control within certain limits which are sufficient to perform laboratory tests on the damper.

Applications of the ideal damper are many. If used in vehicle suspensions, there would result a ride performance vastly improved over that of any damper presently used. Even in the use of air springs (12), the principles of ideal damping could be incorporated in the design of the air control valve. For vibration isolation of physically small components, the principles could be incorporated in the design of the component housing.

It is concluded from this study that the nonlinear ideal damper represents heretofore unrealizable improvement in vibration damping. This is based on the comparison of its superior performance to the performance of the conventional and other damping systems presented herein.

APPENDIX A

ELECTRONIC SWITCH

I Introduction

In the study of the ideal damper, an electronic "on-off" switch, Fig. A-1, was incorporated in the GAP/R Electronic Analog (18) to control that portion of the damping force which was in addition to the residual damping force. The latter was included in the system continually and the relative velocity signal voltage was introduced directly to the D. C. amplifier which represented the coefficient of residual damping, $C_{d(res)}$. The same relative velocity signal voltage was passed through the electronic switch before being introduced to the D. C. amplifier which represented the coefficient of additional damping, $C_{d(add)}$. The sum of the outputs of the two amplifiers then represented the total system damping force. Effectively, the instantaneous magnitude of the system coefficient of damping, C_d, was one of two values: $C_d = C_{d(res)}$ when the switch was "off", and $C_d = C_{d(res)} + C_{d(add)}$ when the switch was "on".

The design of the switch was provided by Mr. Sidney A. Wingate of the GPS Instrument Co. of Boston, Massachusetts, and is an experimental design for a switch to be developed by that company. The switch consists of four basic sections: a bi-stable multivibrator circuit, a diode voltage limiter circuit, a cathode-follower drive circuit, and a diode bridge circuit. The first three sections were installed on one chassis base and the diode bridge circuit was incorporated in the output of a chopper-stabilized K-3A summing component of the electronic analog.

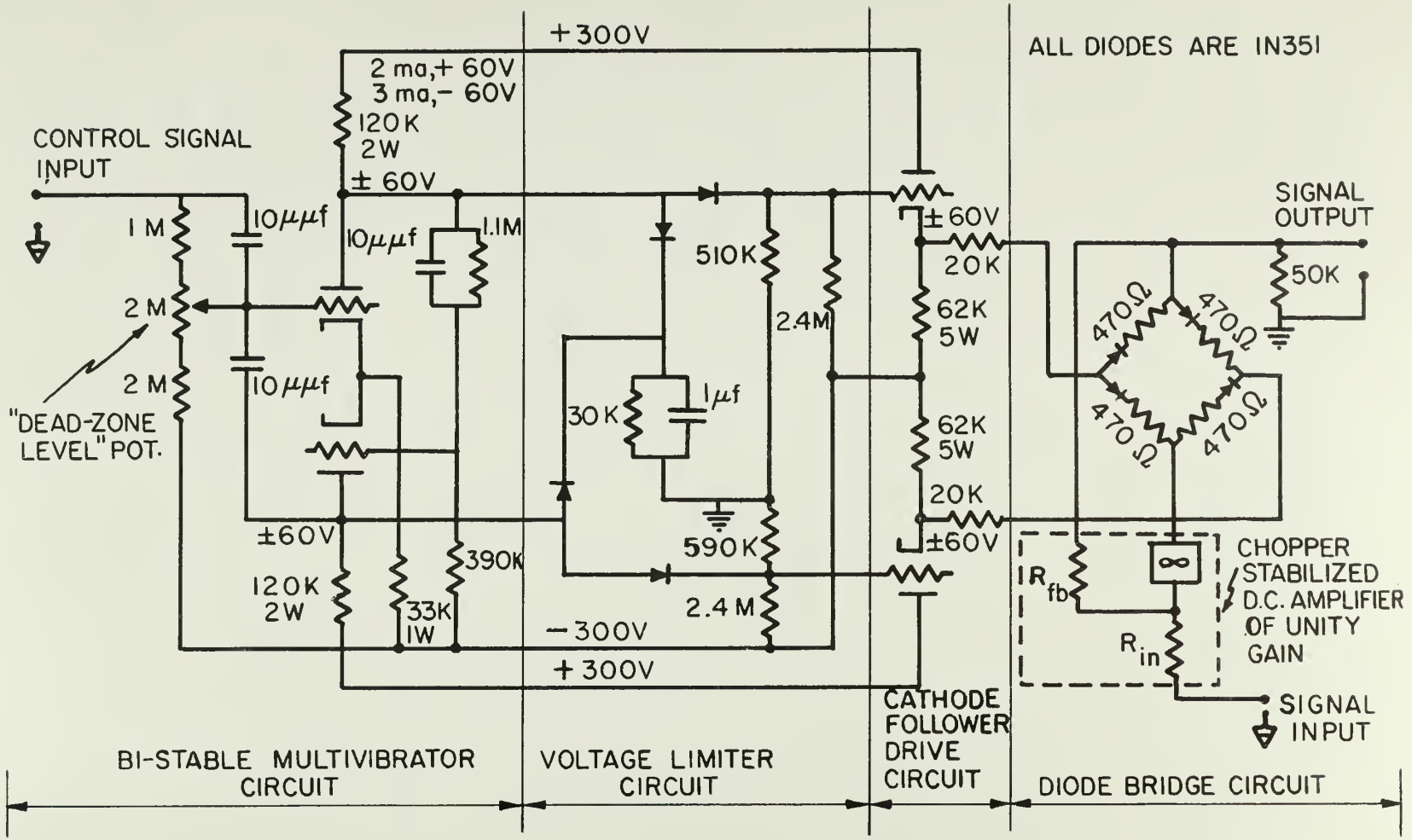

Fig. A-1 Electronic Switch Circuit

II General Operation

The polarity and magnitude of the output voltage of the bi-stable multivibrator is dependent on the grid-cathode potential relative to the plate-cathode potential of the control half of the 12 AY 7 tube (Fig. A-1).

The multivibrator output voltage is limited to the same magnitude in both polarities by the diode limiter circuit and applied to the grids of the cathode-follower drive circuit. The output voltage of the cathode-follower circuit is applied across the diode bridge. The polarity of this voltage, established by the polarity of the vibrator output voltage, determines whether or not the bridge conducts. In a balanced bridge, any signal applied at one midpoint of the bridge will appear at the other midpoint only when the bridge is conducting. Thus a controlled change-in-state of the bridge gives the desired "switching" action and is accomplished by applying the required control signal voltage to the control grid of the bi-stable multivibrator.

III Investigation

A. Bi-Stable Multivibrator Circuit

The circuit is that of a conventional bi-stable multivibrator with the following modifications. The polarity of the multivibrator output voltage (the potential between the two plates) in the static state is determined by the control grid-cathode bias, accomplished manually by adjusting the control grid potentiometer, Fig. A-1. With the magnitude and sign of this bias set, the control signal voltage must be such as to drive the control grid voltage to its switch-over value, thus reversing the polarity of the output voltage. In this design, the cathode remains at approximately -195 volts, but the plate voltage changes from -60 volts during conduction to +60 volts during cut-off. This 120-volt difference in plate-cathode potential results in the switch-over value of control grid voltage being different for cut-off than for

cut-on. Since the larger value of plate-cathode potential exists during conduction, the switch-over voltage required to change from "on" to "off" is lower than that required to change from "off" to "on".

The actual values of the two switch-over voltages depend on the control grid bias, but the difference between the two values is always 20 volts. This constitutes a control signal "dead zone". Therefore, the cycle of the control signal voltage must have a voltage difference exceeding 20 volts in order for the switch to cycle accordingly. This is presented graphically in Fig. A-2. The potential level of the mid-value, as adjusted by the grid bias potentiometer, could be set at any value between ±50 volts.

B. Diode Limiter Circuit

The diode limiter circuit limits the magnitude of multivibrator output voltage to 60 volts in both polarity states and applies this voltage to the grids of the cathode-follower drive circuit.

C. Cathode-Follower Drive Circuit

The polarity of the cathode-follower output voltage (i.e., the potential between cathodes) is determined by the polarity of the voltage applied to the grids, namely, the multivibrator output voltage. The magnitude of the cathode-follower output potential in both polarity states is 120 volts. It must be balanced with respect to zero when applied to the diode bridge.

D. Diode Bridge Circuit

The diodes are arranged as shown in Fig. A-1. It is necessary to ensure that the forward resistance of each branch is the same and that the backward resistance of each branch is the same since any unbalance between branches results in a voltage appearing in the output, giving an erroneous output signal. The cathodes of the cathode-follower must be balanced for the same

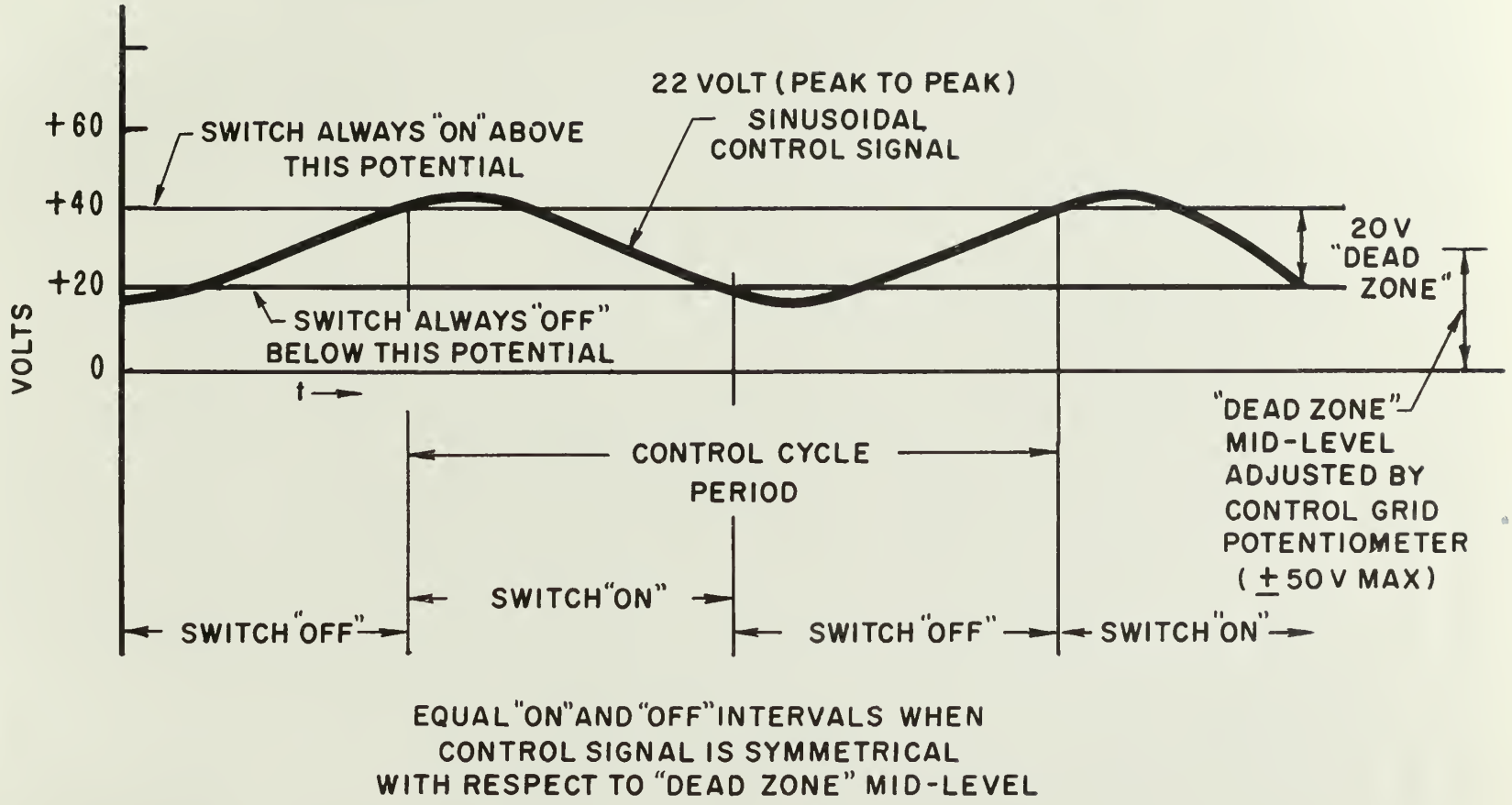

Fig. A-2 Electronic Switch Control Characteristics; Effect of "Dead Zone"

reason. This erroneous output signal would appear in both the "on" and "off" states. In the switch under investigation the balance was satisfactory.

The magnitude of the individual bias of each diode limits the magnitude of the signal which can be controlled, because the polarity of the input signal is always in opposition to that of the bias on one or the other of the adjacent diodes.

The maximum signal magnitude possible in the analog computer is 50 volts, therefore the value of the individual diode bias was selected to be 60 volts. This requires that the cathode-follower output potential be 120 volts.

IV Results and Recommendations

In the multivibrator, the voltage width of the "dead zone" is a function of the tube characteristics and of the plate voltage swing. It is desirable to have the width as narrow as possible but this must be compromised with positive vibrator action. For this switch design, the "dead zone" has a width of 20 volts. This requires that the control signal voltage be amplified to ensure that the control signal cycle has a potential difference of at least 20 volts. The magnitude of control signal voltage to which the switch is to be sensitive determines the degree of amplification required. It is recommended that a variable gain amplifier to accomplish this be an integral part of the switch.

The potentiometer for manually setting the level of the "dead zone" proved extremely useful in the investigative procedures. By turning a knob, a definite "on" or "off" state of the switch can be easily selected. During computation, this facilitates checking and comparison of the computer solution and of the operation of the individual computer components. It is to be noted that this was possible only because the maximum amplified control signal did not exceed ±50 volts and this is not sufficient for a switching cycle when the mid-level of the "dead zone" is set at ±50 volts.

The switch functions as designed in the "off" state, but for an undetermined reason the input signal voltage, in passing through the switch while "on", was clipped at +8 volts and -26 volts. Thus it passes undistorted a maximum signal of 33 volts, peak to peak, if the signal is biased by approximately -9 volts. The K-3A summing component contains a provision for accomplishing this bias. The clipping of the signal can be corrected by improvement in design. As used in the problem, a bias on the signal could not be tolerated, thus the maximum signal into the switch was limited by this clipping to ±8 volts. The clipping did not prevent its use since ±8 volts is a sufficient voltage magnitude for computation. The signal limits were maintained by proper scaling of the problem forcing-function input voltage.

When the diode bridge connections to the cathode-follower were reversed so that the other polarity state caused bridge conduction, it was found that the control signal appeared in the switch output. Since this was not tolerable, the switch could be used only in a one-way "on-off" mode. Redesign of the circuit would correct this defect and permit use of two oppositely directed bridges allowing a versatile two-way "on-off" mode or a diverting mode.

Fig. A-3 is illustrative of the switching action in which some bias is applied to the input signal. In addition, the "dead zone" level is changed relative to the sinusoidal control signal voltage, to vary the "on" and "off" times. For Figs. A-3(a) and (b) the "on" and "off" times are approximately equal.

Fig. A-3(c) shows the "dead zone" effect. Effectively, what is seen is the portion of the control signal (which is also the input signal in Figs. A-3(c) and (d)) which causes the switch to be "on".

Fig. A-3(d) emphasizes the lack of any phase shift or attenuation in the signal in passing through the switch. The figure

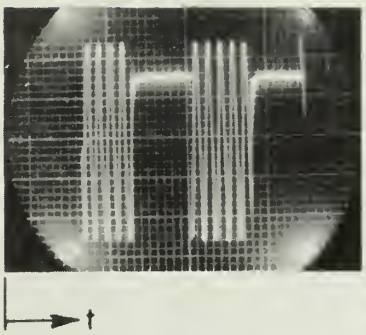

(a) 1500 cps INPUT AS MODIFIED BY 150 cps CONTROL SIGNAL.

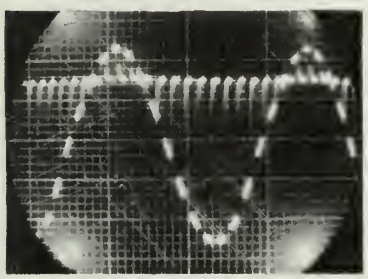

(b) 55 cps INPUT AS MODIFIED BY 550 cps CONTROL SIGNAL.

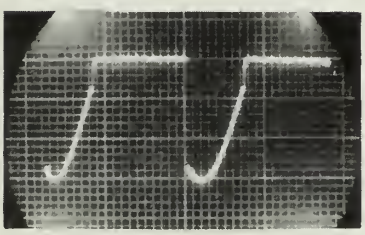

(c) 150 cps INPUT AS MODIFIED BY SAME 150 cps CONTROL SIGNAL.

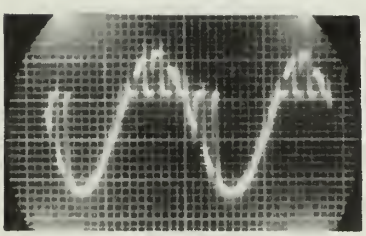

(d) FIG. A-3 (c) AND ITS CONTROL SIGNAL DISPLAYED SIMULTANEOUSLY.

Fig. A-3 Electronic Switch Performance; Sinusoidal Input and Control Signal

shows the output superimposed on the input by use of a micro-switch relay.

Fig. A-3(e) demonstrates the positive switch action for an "impulse" control signal.

In Figs. A-4(a) through (d), maximum and minimum "on-off" time periods, relative to the sinusoidal control signal period, are shown. Fig. A-5 explains Fig. A-4(a) graphically. The control signal was 135 volts peak to peak. The magnitude of the control voltage affects the relative period since the latter is a function of rise (and fall) time through the "dead zone".

The time constant of the output signal when the switch changes state is approximately three micro-seconds. The transient can be noticed in Figs. A-4(c), (d), and (e). Thus it requires approximately ten micro-seconds after the switch is turned "on" for the output to become practically identical to the input. Correspondingly, when turned "off", the output reaches zero in about ten micro-seconds. The effect in the problem under investigation was negligible except at frequencies above 3 KC. In this region, however, the problem was limited by other factors.

In this study the switch was used as a signal "passing" switch. Attempts to connect it into the problem for use as a signal by-pass "shorting" switch were unsuccessful. It is recommended that provision be made for such use since this would increase its versatility and eliminate the effect of any induced signal modification.

With the clipping corrected, and a control signal amplifier incorporated, the design should be satisfactory for use as a fast switching device.

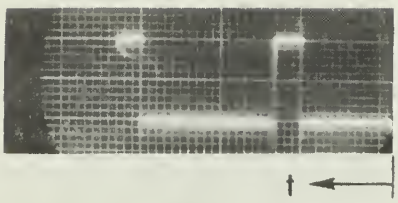

(a) MAXIMUM SWITCH "ON" TIME (85% OF CONTROL SIGNAL PERIOD) FOR 150 cps CONTROL SIGNAL.

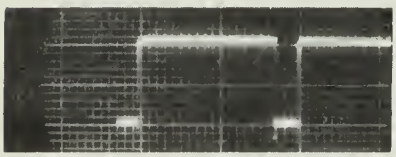

(b) MINIMUM SWITCH "ON" TIME (15% OF CONTROL SIGNAL PERIOD) FOR 150 cps CONTROL SIGNAL.

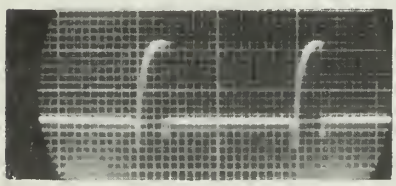

(c) MAXIMUM SWITCH "ON" TIME (85% OF CONTROL SIGNAL PERIOD) FOR 1500 cps CONTROL SIGNAL.

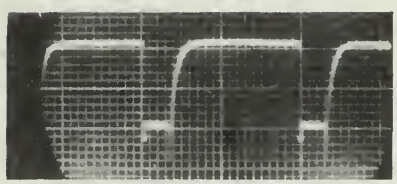

(d) MINIMUM SWITCH "ON" TIME (15% OF CONTROL SIGNAL PERIOD) FOR 1500 cps CONTROL SIGNAL.

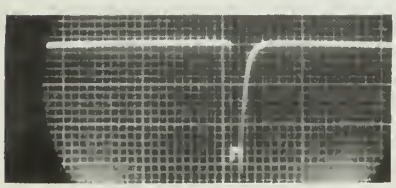

(e) SWITCH "ON" TIME (50 MICRO SECONDS) FOR IMPULSE CONTROL SIGNAL.

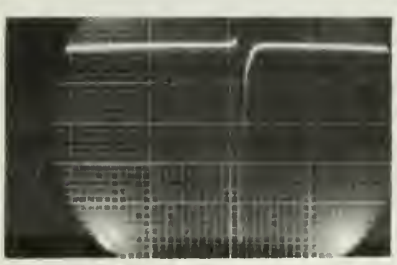

(f) IMPULSE CONTROL SIGNAL FOR (e).

Fig. A-4 Electronic Switch Performance; D-C Voltage Input, Sinusoidal and Impulse Control Signals

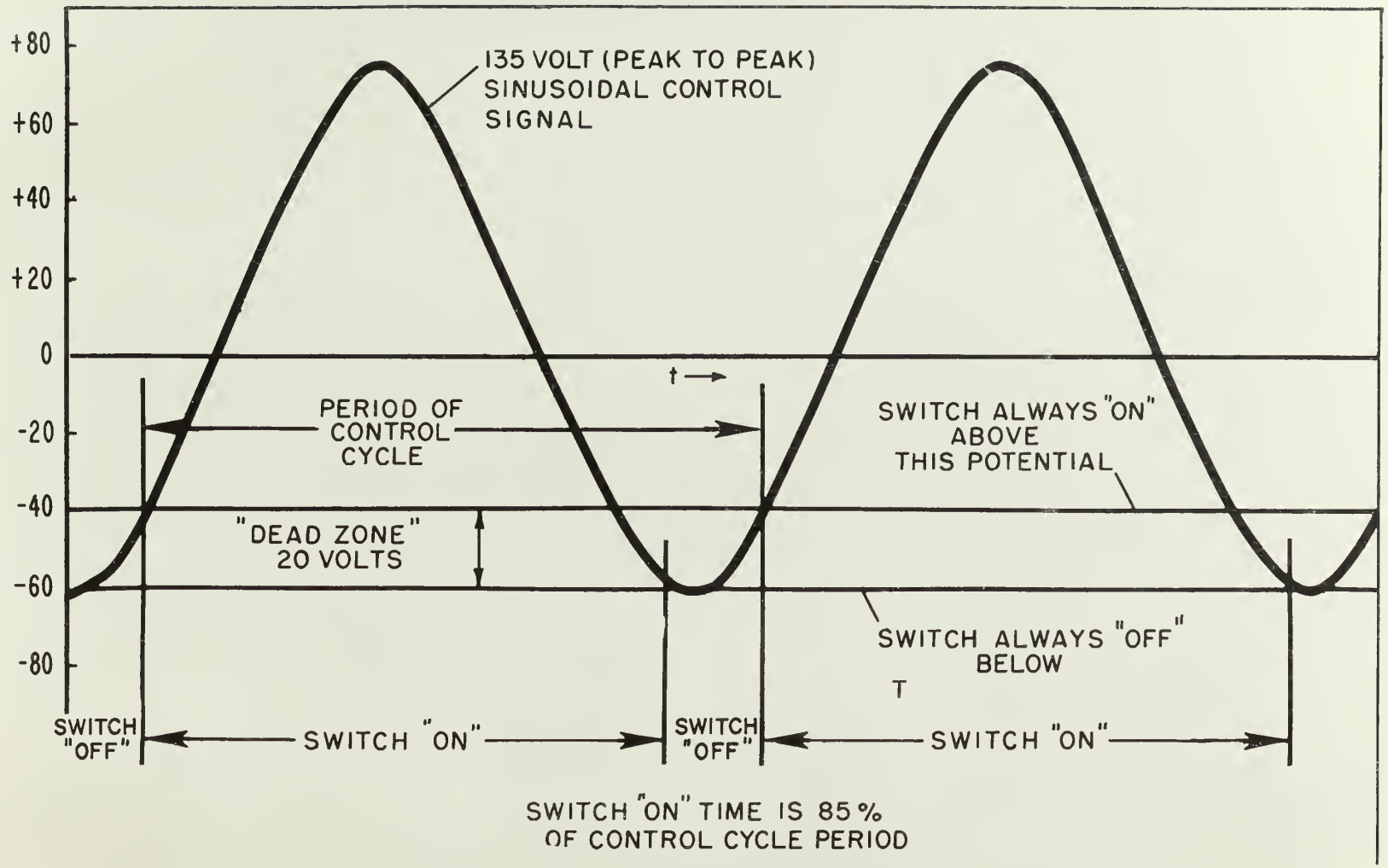

Fig. A-5 Electronic Switch Control Characteristics; Effect of Control Signal on "On-Off" Intervals

APPENDIX B

DESIGN OF VELOCIMETER AMPLIFICATION STAGE

I. PERFORMANCE FUNCTION FOR SINGLE DEGREE OF FREEDOM VELOCIMETER

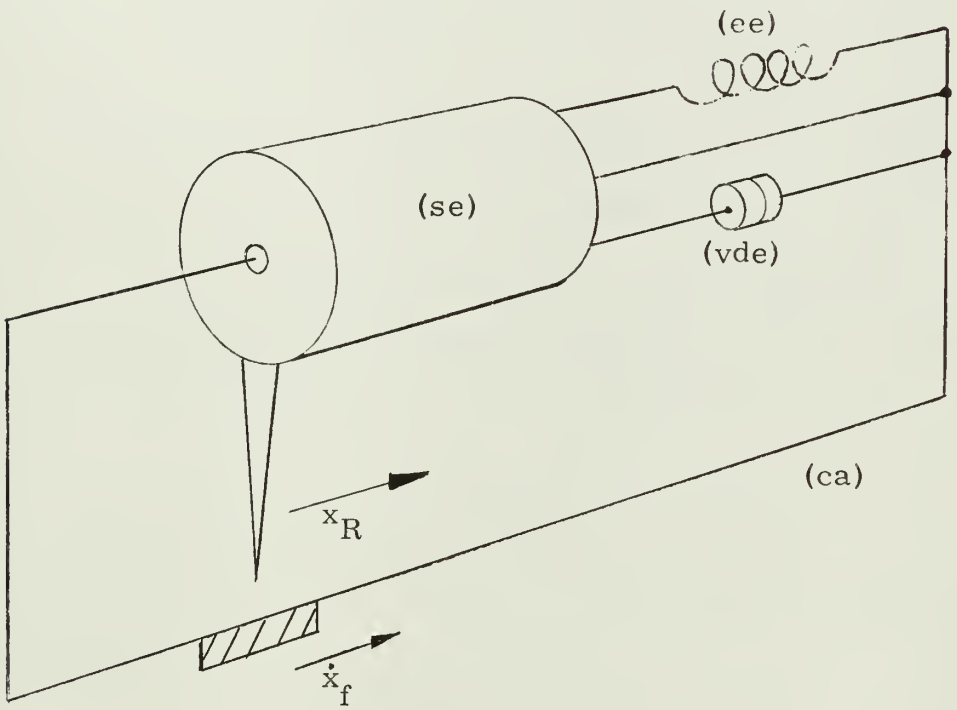

Fig. B-1 Essential Parts of Single Degree of Freedom Seismographic System

Definition of symbols used in Appendix B, Parts I and II.

(as) - amplification stage

(ca) - case

$Cd=C_{(vde)}$ - viscous damping coefficient

(ee) - elastic element

(is) - inner sleeve

$k=k_{(ee)}$ - coefficient of elasticity

m - m_1+m_2

m_1 - mass of spool

m_2 - mass of fluid

$m=m_{(se)}$ - mass of seismic element

(se) - seismic element

$t_{(va)}$ - characteristic time of value

(v) - velocimeter

(va) - valve

(vde) - viscous damping element

$x_{(is)}$ - displacement of inner sleeve

Numerical values used for velocimeter design:

A - Area between spool and case; of thickness (t)
$= 10.9 \times 10^{-4}$ ft.^{2}
$= .157$ in.^{2}

m - $m_1+m_2 = 10^{-4}$ slugs

t - thickness between lands of spool and cylinder
$= .004$ in.
$= .00033$ ft.

V_f - Volume of fluid in spool cylinder $= 9.88 \times 10^{-6}$ ft.^{3}

V_s - Volume of spool $= 4.35 \times 10^{-6}$ ft.^{3}

η - Kinematic viscosity $= .050 \frac{\text{lb.-sec.}}{\text{ft.}^2}$

ρ_f - Density of fluid $= 78.5 \frac{\text{lb.}}{\text{ft.}^3}$

ρ_s - Density of spool $= 490 \frac{\text{lb.}}{\text{ft.}^3}$

Geometrical Relationships:

$$x\,[I-(se)] = x\,[I-(ca)] + x\,[(ca)-(se)]$$

$$x_R = x\,[(ca)-(se)] = \text{relative displacement}$$

$$x_f = x\,[I-(ca)] = \text{forcing displacement}$$

Assumptions:

1. Neglect Coulomb friction
2. Damping fluid is incompressible
3. Spring force is a linear function of displacement
4. Damping force is a linear function of velocity

By equating the summation of forces acting on the seismic element to zero, the equation of motion can be written.

(Inertia reaction force) + (Viscous damping) + (Elastic Element) = 0
Force Force

$$-m\,\ddot{x}\,[I(se)] - C_d\,\dot{x}\,[(ca)-(se)] - k\,x\,[(ca)-(se)] = 0 \qquad (1)$$

Dividing through by m, substituting geometrical relationships and rearranging terms gives:

$$\ddot{x}_R + \frac{C_d}{m}\,\dot{x}_R + \frac{k}{m}\,x_R = -\ddot{x}_f \qquad (2)$$

Comparing Equation (2) to the standard forms found in Chapter 19 of (9) gives:

$$\ddot{x}_R + 2\zeta\,\omega_n\,\dot{x}_R + \omega_n^2\,x_R = -\ddot{x}_f \qquad (3)$$

where $\omega_n = \sqrt{k/m}$; $\zeta = \dfrac{C_d}{2\sqrt{km}}$

In operational form, Equation (3) becomes:

$$(p^2 + 2\zeta\,\omega_n p + \omega_n^2)\quad x_R = -\,p^2 x_f \tag{4}$$

where $p = d/dt$

The performance function for the seismographic system as a velocimeter, forcing velocity as input and relative displacement output, becomes

$$\left[PF\right]_v \left[\dot{x}_f;\, x_R\right] = \frac{-S_v p}{\left[\left(\frac{p}{\omega_n}\right)^2 + \frac{2\zeta}{\omega_n} p + 1\right]} \tag{5}$$

II. DESIGN OF AMPLIFICATION STAGE

The functional diagram for the velocimeter amplification stage is seen in Fig. B-2.

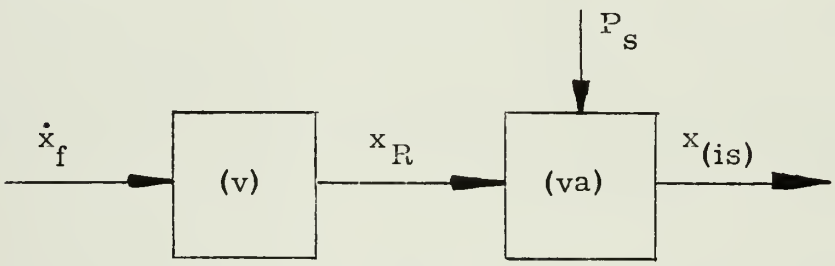

Fig. B-2

The performance functions for the components in Fig. B-2 are:

$$\left[PF\right]_v \left[\dot{x}_f;\, x_R\right] = \frac{-S_{(v)}(p)}{\left(\frac{p}{\omega_n}\right)^2 + \frac{2\zeta}{\omega_n} p + 1} \tag{6}$$

$$\left[PF\right]_{(va)} \left[x_R; x_{is}\right] = \frac{S_{(va)} \left[x_R; x_{is}\right]}{1 + t_{(va)} p} \tag{7}$$

$$\left[PF\right]_{(as)} \left[\dot{x}_f; x_{(is)}\right] = \frac{-(S_v)(S_{va}) \quad p}{\left[\left(\frac{p}{\omega_n}\right)^2 + \frac{2\zeta}{\omega_n} p + 1\right]\left[1 + t_{(va)} p\right]} \tag{8}$$

The lag introduced by $t_{(va)}$ can be compensated for by tuning the natural frequency of the velocimeter above that of the normal forcing frequency. This can be accomplished by increasing the spring stiffness. This tuning forces the velocimeter into the accelerometer range, thus putting a lead into the system to counteract the lag $t_{(va)}$.

Fig. B-3 shows the essential parts of the velocimeter.

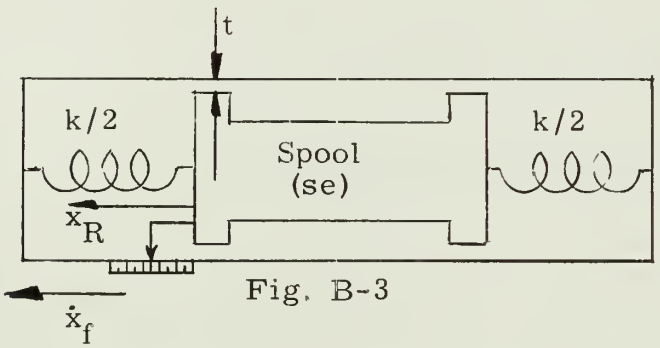

Fig. B-3

The desired sensitivity of the velocimeter s_v is .0006 ft./ft./sec. and for a first approximation the spring force is neglected, thus

$$m\ddot{x}_f + C_d\dot{x}_R = 0 \tag{10}$$

Integrating once and solving for S_v

$$S_v \left[\dot{x}_f, x_R\right] = \frac{x_R}{\dot{x}_f} = \frac{m}{C_d} = .0006 \text{ ft./ft./sec.} = \frac{.007 \text{ inches}}{\text{ft./sec.}}$$

Based on the selected dimensions, page 70, the value for m was computed to be 10^{-4} slugs and includes the mass of the spool plus the mass of the fluid which will be displaced with the spool. With this value for m, the required cd can be computed.

$$C_d = \frac{m}{s_v} = \frac{10^{-4}}{.0006} = .165 \frac{\text{lb.-sec.}}{\text{ft.}}$$

Assuming a value for ω_n of 8 rad./sec. and from

$$\omega_n^2 = k/m$$

the spring stiffness k can be found

$$k = \omega_n^2 m = 64 \times 10^{-4} \text{ lb./ft.}$$

$$= .0064 \text{ lb./ft. or } .1 \text{ gm/cm.}$$

Since the damping ratio $\zeta = \frac{cd}{2\sqrt{km}}$

$$\zeta = \frac{.165}{2\sqrt{64 \times 10^{-4} \times 10^{-4}}} = 103$$

Wt. of spool = 1 gram

In the actual velocimeter (b), using castor oil,

$$C_d = \frac{\eta A}{t} = \frac{.050 \quad 10.9 \times 10^{-4}}{\frac{.004}{12}} = .165$$

which gives a damping ratio ζ:

$$\zeta = \frac{.165}{2\sqrt{64 \times 10^{-4} \times 10^{-4}}} = 103$$

From Fig. 35-20 p. 695, Vol. III of (9)

$$D\left[PR\right](ss)\left[x_f ; x_R\right] = -.0015; \quad .1 < \frac{\omega_f}{\omega_n} < 10$$

APPENDIX C

GRAPHICAL APPROXIMATION OF SOLUTION OF SECOND ORDER SYSTEM WITH IDEAL DAMPING

The basic nonlinear equation of motion for the ideal damper (equation (2-3), page 22) is:

$$-m\ddot{x}_o + \left[C_d(\dot{x}_{in} - \dot{x}_o)\right] + k(x_{in} - x_o) = 0$$

where: $C_d = C_{d_{(res)}}$ when $\dot{x}_o$ and $(\dot{x}_{in} - \dot{x}_o)$ have same sign

$C_d = C_{d_{(res)}} + C_{d_{(add)}}$ when $\dot{x}_o$ and $(\dot{x}_{in} - \dot{x}_o)$ have opposite signs.

A graphical first approximation to the solution of this (1, 0; 0, 1, 2) equation may be carried out as follows:

1. Modify the basic equation to:

$$-m\frac{\ddot{x}_o}{X_{in}} + \left[C_d\left(\frac{\dot{x}_{in}}{X_{in}} - \frac{\dot{x}_o}{X_{in}}\right)\right] + k\left(\frac{x_{in}}{X_{in}} - \frac{x_o}{X_{in}}\right) = 0 \qquad \text{(C-1)}$$

where: $C_{d_{low}} = C_{d_{(res)}}$ when $\dot{x}_o$ and $(\dot{x}_{in} - \dot{x}_o)$ have same sign

$C_{d_{high}} = C_{d_{(res)}} + C_{d_{(add)}}$ when $\dot{x}_o$ and $(\dot{x}_{in} - \dot{x}_o)$ have opposite signs.

and where: $x_{in} = X_{in} \sin\omega t$

Thus

$$\frac{x_{in}}{X_{in}} = \sin\omega t \qquad \text{(C-2)}$$

$$\frac{\dot{x}_{in}}{X_{in}} = \omega\cos\omega t \qquad \text{(C-3)}$$

$$\frac{\ddot{x}_{in}}{X_{in}} = -\omega^2 \sin\omega t \qquad \text{(C-4)}$$

2. Select parameters of $\zeta = \frac{C_d}{2\sqrt{km}}$, $\omega_n = \sqrt{\frac{k}{m}}$, and $\beta = \frac{\omega_f}{\omega_n}$ and plot equations (C-2), (C-3), and (C-4).

3. Assume that the phase shift, ϕ, of the nonlinear (1, 0;0, 1, 2) system is that of a linear system with a damping ratio between that of ζ_{low} and ζ_{high}.

4. Since the design performance is to approach perfect damping performance with a (0;0, 1, 2) type equation of motion, assume that the amplitude ratio is that of perfect damper with a damping ratio between that of ζ_{low} and ζ_{high}.

5. Based on these assumptions, then

$$x_o = (AR) X_{in} \sin(\omega t - \phi)$$

and

$$\frac{x_o}{X_{in}} = (AR)\sin(\omega t - \phi) \qquad \text{(C-5)}$$

$$\frac{\dot{x}_o}{X_{in}} = \frac{d}{dt}\left(\frac{x_o}{X_{in}}\right) \qquad \text{(C-6)}$$

$$\frac{\ddot{x}_o}{X_{in}} = \frac{d}{dt}\left(\frac{\dot{x}_o}{X_{in}}\right) \qquad \text{(C-7)}$$

6. As a starting point, take x_o as zero going positive at ωt corresponding to the phase shift.

7. At this point, assume $\dot{x}_o$ is maximum positive, and $\ddot{x}_o$ is zero going negative. This reduces the modified basic equation to:

$$\frac{\dot{x}_{out}}{X_{in}} = \frac{\dot{x}_{in}}{X_{in}} + \frac{k}{C_d}\left(\frac{x_{in}}{X_{in}}\right)$$

8. At this point, determine the values of $\frac{\dot{x}_{in}}{X_{in}}$ from (C-2) and $\frac{\dot{x}_{in}}{X_{in}}$ from (C-3).

9. From the values in 8. determine which C_d is active.

10. Solve for $\frac{\dot{x}_o}{X_{in}}$ in 7.

11. For plotting the graphical solution, select intervals of ωt. The values computed at a particular ωt are denoted by a subscript number corresponding to that number of intervals from the starting point.

12. Thus $\left.\frac{x_{out}}{X_{in}}\right]_0 = 0$, $\left.\frac{\dot{x}_{out}}{X_{in}}\right]_0$ from 10., $\left.\frac{\ddot{x}_{out}}{X_{in}}\right]_0 = 0$

and are plotted.

13. Plot the value of $\left.\frac{x_{out}}{X_{in}}\right]_1$. This is determined by equation (C-5).

14. Plot the value of $\left.\frac{\dot{x}_{out}}{X_{in}}\right]_1$. This is determined by equation (C-6) and is accomplished by measuring the slope of $\left.\frac{x_{out}}{X_{in}}\right]_1$.

15. Plot the value of $\left.\frac{\ddot{x}_{out}}{X_{in}}\right]_1$. This is determined by

equation (C-7) and is accomplished by measuring the slope of $\left.\frac{\dot{x}_{out}}{X_{in}}\right]_1$.

16. The steps so far give first values for the first approximation. To refine the first approximation, the values of $\left.\frac{x_{out}}{X_{in}}\right]_1$, $\left.\frac{\dot{x}_{out}}{X_{in}}\right]_1$, $\left.\frac{\ddot{x}_{out}}{X_{in}}\right]_1$, $\left.\frac{x_{in}}{X_{in}}\right]_1$, and $\left.\frac{\dot{x}_{in}}{X_{in}}\right]_1$ are substituted in the modified basic equation (C-1), and adjusted accordingly. The acceleration value is the most critical.

17. At successive intervals, steps 13. through 16. are repeated. The effect of assuming $\left.\frac{\ddot{x}_o}{X_{in}}\right]_0 = 0$ is pronounced, and a compromise between the value of (AR) used and the value of $\left.\frac{\dot{x}_o}{X_{in}}\right]_0$ from 10., as compared to, $\left.\frac{\dot{x}_{in}}{X_{in}}\right]_0$ must be made.

Successive graphic computations should give an approximate solution.

BIBLIOGRAPHY

1. "Vibration Problems in Engineering," by Timoshenko, D. Van Nostrand Co., Inc., New York, N.Y., Second Edition, 1937.

2. "Vibration Prevention in Engineering," by Arthur L. Kimball, John Wiley and Sons, Inc., New York, N.Y., 1932.

3. "Vibration of Rail and Road Vehicles," by B. S. Cain, Pitman Publishing Corp., New York, N.Y., 1940.

4. "Damping in Suspensions," by B. E. O'Connor, SAE Journal, August 1946.

5. SAE Editorial Report, SAE Journal, March 1957. p. 86.

6. "Band-Pass Shock and Vibration Absorbers for Application to Aircraft Landing Gear," by Emanuel Schnitzer, NACA Technical Note 3803, October 1956.

7. "New Features in Shock Absorbers with Inertia Control," by C. H. Kindl, SAE Transactions 1933. p. 172.

8. "The Modern Chassis," by Hank Elfrink, Floyd Clymer Publisher, Los Angeles, California, 1951. p. 66.

9. "Instrument Engineering," by Charles S. Draper, Walter McKay, and Sidney Lees, McGraw Hill Book Company, Inc., New York, N.Y., First Edition, Vol. I, 1952, Vol. II, 1953, and Vol. III, 1955.

10. "Fluid Mechanics," by R. A. Dodge and M. J. Thompson, McGraw Hill Book Company, Inc., New York, N.Y., 1937.

11. "Catalog and Manual on GAP/R High-Speed, All Electronic Analog Computer for Research and Design," G. A. Philbrick Researchers, Inc., 1951.

12. "Air and Heavy Vehicle Suspensions," by Roy W. Brown, SAE Journal, June 1955 p. 37.

Thesis 36043
E56 Erb
The principles and analog studies of an ideal vibration damper.